Geomaterials (Petrology)

Serpentinization of abyssal peridotites at mid-ocean ridges

Catherine Mével

Laboratoire de Géosciences marines, CNRS UMR 7097, IPGP, 4, place Jussieu, 75252 Paris cedex 05, France

Abstract

Serpentinites are an important component of the oceanic crust generated in slow to ultraslow spreading settings. In this context, the MOHO likely corresponds to a hydration boundary, which could match the 500 °C isotherm beneath the ridge axis. Textures from serpentinites sampled in ridge environments demonstrate that most of the serpentinization occurs under static conditions. The typical mineralogical association consists of lizardite ± chrysotile + magnetite ± tremolite ± talc. Despite the widespread occurrence of lizardite, considered as the low temperature serpentine variety, oxygen isotope fractionation suggests that serpentinization starts at high temperature, in the range of 300–500 °C. The fluid responsible for serpentinization is seawater, possibly evolved by interaction with the crust. Compared with fresh peridotites, serpentinites are strongly hydrated (10–15% H_2O) and oxidized. Serpentinization, however, does not seem to be accompanied by massive leaching of major elements, implying that it requires a volume increase. It results in an increase in chlorine, boron, fluorine, and sulfur, but its effect on other trace elements remains poorly detailed. The presence of serpentinites in the oceanic crust affects its physical properties, in particular by lowering its density and seismic velocities, and modifying its magnetic and rheological properties. Serpentinization may activate hydrothermal cells and generate methane and hydrogen anomalies which can sustain microbial communities. Two types of hydrothermal field have been identified: the Rainbow type, with high temperature (360 °C) black smokers requiring magmatic heat; the low temperature (40–75 °C) Lost City type, by contrast, can be activated by serpenintization reactions. ***To cite this article: C. Mével, C. R. Geoscience 335 (2003).***
© 2003 Académie des sciences. Published by Éditions scientifiques et médicales Elsevier SAS. All rights reserved.

Résumé

Serpentinisation des péridotites abyssales aux dorsales océaniques. Les serpentinites représentent un constituant important de la croûte océanique formée aux dorsales lentes et ultralentes. Dans ce contexte, le MOHO pourrait correspondre à un front d'hydratation et éventuellement à l'isotherme 500 °C sous l'axe. L'observation des textures des serpentinites échantillonnées aux dorsales montre que l'essentiel de la serpentinisation a lieu en régime statique. L'association minérale type comprend lizardite ± chrysotile + magnetite ± tremolite ± talc. Malgré la présence de lizardite considérée comme l'espèce serpentineuse de basse température, le fractionnement isotopique de l'oxygène montre que la serpentinisation commence à température élevée, de l'ordre de 300 à 500 °C. Le fluide responsable de la serpentinisation est majoritairement l'eau de mer, qui a pu évoluer par réaction avec la croûte. Par rapport aux péridotites fraîches, la serpentinisation se traduit par une hydratation massive et l'oxydation du fer. Elle ne semble pas être accompagnée d'échanges importants en éléments majeurs, ce qui implique qu'elle entraîne une augmentation de volume. Elle s'accompagne d'un enrichissement en chlore, bore, fluor, soufre. Son effet sur les autres éléments en traces reste mal contraint. La présence de serpentinites dans la croûte océanique affecte ses

E-mail address: mevel@ipgp.jussieu.fr (C. Mével).

propriétés physiques, en particulier en abaissant la densité et les vitesses de propagation des ondes sismiques, et en modifiant ses propriétés magnétiques et rhéologiques. La serpentinisation peut activer des cellules de convection hydrothermales et provoquer des anomalies de méthane et d'hydrogène, capables d'alimenter des communautés microbiennes. Deux types de champs hydrothermaux ont été mis en évidence : le type « Rainbow », à fumeurs noirs de haute temperature (360 °C), nécessite un apport de chaleur magmatique ; le type « Lost City » de basse température (40–75 °C) peut être activé par la seule réaction de serpentinisation. ***Pour citer cet article : C. Mével, C. R. Geoscience 335 (2003).***

Version française abrégée

La présence de péridotites serpentinisées sur le plancher océanique est connue depuis longtemps mais ce n'est que récemment, grâce à une meilleure connaissance de la géologie des fonds océaniques, que l'on a commencé à comprendre les mécanismes responsables de leur mise à l'affleurement. Les serpentinites sont un constituant majeur de la croûte océanique formée aux dorsales lentes et ultralentes. Elles affleurent également à la transition continent-océan, où leur présence est le résultat de la déchirure océanique dans un contexte de faible production magmatique (par exemple la marge Ibérique). Enfin, on les rencontre au niveau des zones de subduction comme la fosse des Mariannes. Elles résultent alors de la remontée diapirique de manteau hydraté provenant soit de la plaque plongeante, soit du coin mantellique susjacent. Dans cette revue ne seront prises en compte que les serpentines des dorsales océaniques, dont la formation est liée aux processus de l'accrétion.

Aux dorsales lentes et ultralentes, la présence d'une lithosphère épaisse rend plus difficile la remontée vers la surface du magma produit par la fusion partielle. De nombreuses études, tant dans la dorsale médio-Atlantique que la dorsale sud-ouest-Indienne et plus récemment la ride de Gakkel dans l'Arctique, ont montré que, dans ce contexte, le magma tend à se focaliser au centre des segments, et les serpentinites affleurent fréquemment dans la vallée axiale aux extrémités des segments. La croûte océanique formée dans cet environnement ne répond pas au modèle PENROSE de lithosphère litée, caractérisé par une superposition de couches (Couche 2 = basaltes, Couche 3 = gabbro et, sous le MOHO, Couche 4 = péridotites mantelliques). Son architecture est hétérogène et varie le long

de l'axe (Fig. 1). Aux extrémités des segments, elle est constituée de péridotites plus ou moins serpentinisées recoupées par des intrusions gabbroïques (Fig. 2). Dans ce contexte, le MOHO, discontinuité sismique qui sépare la croûte du manteau, pourrait correspondre à un front de serpentinisation. Dans un contexte de lithosphère épaisse, les péridotites serpentinisées peuvent être également mises à l'affleurement par le jeu de grandes failles à faible pendage. Cette nouvelle perspective sur le fonctionnement des dorsales lentes montre que les serpentinites n'y sont pas cantonnées aux grandes failles transformantes, mais représentent un constituant majeur de la croûte. Au contraire, aux dorsales rapides, le modèle PENROSE semble s'appliquer. Les péridotites serpentinisées n'affleurent que dans des contextes tectoniques particuliers.

Les nombreux travaux effectués sur les péridotites serpentinisées collectées aux dorsales, et en particulier dans le cadre du programme de forages océaniques ODP, montrent des caractères constants dans les textures et la minéralogie. Le taux de serpentinisation est généralement élevé (80–100%). La serpentinisation a eu lieu en régime statique (Fig. 3A), même si les veines sont nombreuses (Fig. 3B et 3G). Les textures originelles des péridotites sont préservées : les olivines sont remplacées par de la serpentine maillée (Fig. 3C et 3D) et les pyroxènes par de la serpentine en bastites (Fig. 3E). Amphibole et talc sont parfois associés aux bastites (Fig. 3F). Les serpentines schisteuses (Fig. 3H) sont rares.

La serpentine, phyllosilicate de silice et magnésium hydraté, est le minéral le plus abondant. Sa formation résulte de l'altération de l'olivine et des pyroxènes par un fluide hydraté, réaction qui produit également de la magnétite et de l'hydrogène. Brucite, divers types d'amphiboles, talc, chlorites, carbonates peuvent éga-

lement être présents. Des trois variétés de serpentine (Fig. 4), la lizardite est la plus fréquente. Le chrysotile lui est parfois associé, mais est surtout présent en veines. L'antigorite est rare. L'abondance de la lizardite semble résulter de sa capacité à accepter les substitutions.

Les conditions de la serpentinisation aux dorsales océaniques sont difficiles à déterminer en l'absence d'indicateurs précis, et parce que les roches montrent la superposition de différents stades. La pression est nécessairement faible puisque la profondeur du MOHO, au-delà duquel les serpentinites ne doivent plus exister, ne dépasse guère les 6 km. Des données expérimentales et thermodynamiques suggèrent des températures décroissantes pour les limites de stabilité respectives de l'antigorite, du chrysotile et de la lizardite (Fig. 5). Cependant, l'abondance de la lizardite est en désaccord avec les températures élevées déduites d'autres indicateurs. Les autres minéraux associés aux serpentines suggèrent généralement des conditions compatibles avec le faciès schiste vert (300–500 °C). Des données plus précises peuvent être obtenues avec le fractionnement des isotopes de l'oxygène (Fig. 6). Mais les courbes de calibration sont encore mal contraintes. Le Tableau 1 résume les résultats obtenus. Ils montrent un grand éventail de températures (de 500 °C à moins de 100 °C), qui suggère une grande diversité dans les conditions de serpentinisation, mais souligne que la serpentinisation commence à haute température (350–500 °C). Les serpentinites contiennent 10–15% d'eau et la phase fluide responsable de la serpentinisation est constituée principalement d'eau de mer. Mais les compositions isotopiques de l'oxygène, de l'hydrogène et du strontium (Fig. 7) suggèrent qu'il s'agit d'eau de mer qui a évolué par réaction avec la croûte.

La serpentinisation, qui s'accompagne d'une forte hydratation, provoque une baisse de la densité qui chute de 3,3 à 2,5. Cette constatation a engendré de nombreux débats concernant les conséquences de la serpentinisation sur les flux d'éléments chimiques : si la baisse de densité a lieu à volume constant, elle est nécessairement accompagnée d'un lessivage massif d'une partie des éléments chimiques ; si elle est accompagnée d'une augmentation de volume, la composition chimique originelle peut être préservée. Les travaux récents effectués sur les serpentinites océaniques suggèrent que les éléments majeurs sont peu affectés

– en dehors de l'hydratation et de l'oxydation du fer, ainsi que de métasomatisme local (formation de talc, rodingitisation), et militent donc plutôt en faveur de la seconde hypothèse. En revanche, certains éléments traces sont très affectés. En particulier, les serpentinites sont enrichies en Cl, B, S, F. Le comportement des terres rares est encore mal contraint, de même que celui de la plupart des isotopes radiogéniques. Ces éléments sont surtout concentrés dans les pyroxènes et en conséquence, les résultats sont certainement fonction de leur comportement au cours de la serpentinisation. Une étude systématique reste à faire pour bien caractériser les flux de matière entre péridotites et eau de mer au cours de la serpentinisation.

La serpentinisation a des conséquences majeures sur les propriétés physiques. Par rapport à une péridotite fraîche, la chute de densité provoque une baisse des vitesses sismiques. Il existe une relation inverse entre le taux de serpentinisation et la densité ainsi que la vitesse de propagation des ondes sismiques (Fig. 8). Ceci explique l'existence du MOHO, même dans le cas où des roches d'origine mantellique (péridotites serpentinisées) affleurent sur le plancher océanique. Dans ce cas, le MOHO doit correspondre à un front d'hydratation voire, dans la mesure où la température maximum de stabilité de la serpentine est de 500 °C, à l'isotherme 500 °C. Les propriétés magnétiques des péridotites sont également affectées. Étant donné que la serpentinisation produit de la magnétite secondaire, les serpentinites acquièrent une magnétisation rémanente naturelle (RMN) et donc peuvent contribuer aux anomalies magnétiques du plancher océanique. Une étude de détail des propriétés magnétiques des serpentinites a cependant montré que l'intensité de la susceptibilité magnétique n'augmentait pas linéairement avec le taux de serpentinisation. En effet, elle dépend de capacité des minéraux serpentineux à incorporer du fer, qui contrôle la quantité de magnétite produite. Enfin, la présence de serpentine modifie les propriétés rhéologiques et donc a une influence sur l'activité tectonique.

Aux dorsales océaniques, la serpentinisation peut activer une circulation hydrothermale. Les premières manifestations de cette activité ont été découvertes sous forme d'anomalies de méthane dans la colonne d'eau, systématiquement associées à des affleurements de serpentinites. La production de méthane est liée à

des réactions de type Fisher-Trops :

$$CO_2 + 4\,H_2 = CH_4 + 2\,H_2O$$
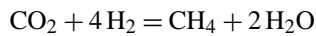
qui font intervenir l'hydrogène produit pendant la serpentinisation.

Plus récemment, de véritables champs hydrothermaux ont été découverts sur les péridotites serpentinisées. Les champs de Logatchev et de Rainbow, respectivement localisés à 14°45N et 36°14N sur la dorsale médio-Atlantique, sont assez semblables à ceux installés sur les basaltes : des fumeurs noirs émettent des fluides chargés en particules à des températures de l'ordre de 360 °C. Ils construisent des cheminées de sulfures et abritent des colonies biologiques. Les fluides ont un faible pH et sont chargés en H_2S et en métaux. Cependant, par rapport aux fluides émis en contexte basaltique, ils ont des teneurs élevées en H^+, résultat des réactions de serpentinisation (Tableau 2). Ils contiennent également des molécules d'hydrocarbures complexes, considérées comme des molécules prébiotiques, qui font de ces sites hydrothermaux des endroits potentiels pour l'apparition de la vie sur Terre. Mais un nouveau type d'activité hydrothermale vient d'être découvert au site de Lost City, à 30°N hors axe de la dorsale médio-Atlantique. Les fluides sont émis à des températures beaucoup plus faibles (40–75 °C), ont un fort pH et de faibles concentrations en H_2S et sont chargés en MgO (Tableau 2). Ils construisent d'énormes cheminées constituées de brucite et de carbonates.

Différents auteurs ont tenté d'estimer si la chaleur produite par la réaction de serpentinisation qui est exothermique peut suffire à activer une circulation hydrothermale. Il ressort des calculs que la seule chaleur dégagée par la serpentinisation ne peut suffire à réchauffer des fluides à des températures de plus de 300 °C et qu'en conséquence, de la chaleur dégagée par des intrusions magmatiques est certainement impliquée à Rainbow comme à Logatchev. En revanche, dans le cas de Lost City, la seule chaleur de serpentinisation pourrait suffire. Les champs hydrothermaux de ce type devraient être fréquents dans la vallée axiale ou hors axe, à condition que l'eau de mer puisse pénétrer dans des péridotites fraîches.

En conclusion, il est maintenant démontré que les serpentinites, résultat de l'interaction des péridotites océaniques avec l'eau de mer, sont un constituant important de la lithosphère océanique formée aux dorsales lentes et ultralentes. La présence de ces serpentinites a des conséquences importantes sur la composition chimique de la lithosphère, mais les flux chimiques globaux résultant de la serpentinisation sont encore mal contraints. Elle modifie également ses propriétés physiques et peut contribuer aux anomalies magnétiques du plancher océanique. Elle implique de réévaluer les budgets magmatiques aux dorsales, dans la mesure où la croûte océanique peut comprendre une certaine proportion de roches d'origine mantellique et donc résiduelles. Des cellules de convection hydrothermale peuvent être activées par la serpentinisation, soit avec la contribution de chaleur dégagée par des intrusions magmatiques, soit sous le simple effet de la réaction exothermique de serpentinisation. Enfin, sur le plan global, la présence de serpentinites riches en eau et en halogènes dans la lithosphère subductée doit avoir des conséquences dans les processus de déshydratation de la plaque plongeante et dans les mécanismes de fusion des magmas d'arcs insulaires.

1. Introduction

The presence of serpentinites on the seafloor has been documented for a very long time. On the basis of this occurrence and of the seismic structure, Hess proposed [73] that oceanic layer 3 consists of a hydrated mantle, i.e. serpentinites, and that the uniform thickness of the ocean crust corresponded to the depth of the 500 °C isotherm at mid-ocean ridges. The increasing knowledge of the oceanic lithosphere has demonstrated that this picture of the ocean crust was certainly extreme, but that serpentinites do represent a significant portion of the crust.

All the abyssal peridotites that crop out on the seafloor are more or less serpentinized. They commonly occur in slow to ultraslow spreading ridge environments. In the early days, when the topography of ridges was not well known, peridotites were dredged mostly from major scarps, which were essentially transform fault walls [22,23,27,28,100], although some also came from the axial valley [7]. It was also recognized that these ultramafic occurred in the Atlantic and Indian oceans, i.e. at slow spreading ridges, but this could be attributed to the higher density of fracture zones in this environment. It was argued that hydration of the underlying mantle peri-

dotites was made possible by the presence of large faults, driving seawater at depth and the outcropping of serpentinites was commonly ascribed to diapiric emplacement, due to the low density of serpentine (2.5 g/cm^3) with respect to the average density of the ocean crust (2.8 g/cm^3) [7,27,28]. It is only during the last 15 years, when the knowledge of the mid-ocean ridge structure improved, that a general understanding for the location of peridotites outcrops has emerged, and it has been recognized that at slow to ultraslow spreading ridges, serpentinized peridotites are an important component of the crust.

Serpentinites also occur in other tectonic settings at the seafloor. They have been recorded at passive margins. Serpentinized peridotites were first documented at the Galicia margin where they form a few km wide and a hundred km long ridge, at the continent-ocean boundary [18]. Further work showed that this ridge is a major feature, which continues south to the Iberian margin [12]. This serpentinite ridge is interpreted as resulting from mantle exhumation due to crustal thinning during the initial stage of rifting. At the continent-ocean transition, the tectonic activity is inferred to favour seawater penetration and serpentinization [20, 21]. The serpentinites exposed at the Galicia and Iberia margins have been drilled by the Ocean Drilling Program during Leg 103 [19] and 149 [134] respectively. A similar mechanism has been invoked to explain the occurrence of serpentinized peridotites at the Tyrrhenian margin, drilled during ODP leg 107 [31]. A similar occurrence of serpentinized peridotites [102] at the southwest Australian margin is interpreted as resulting from the rifting between Australia and Antarctica [13]. However, serpentinites also occur at active margins. They have been dredged at the Tonga trench [61] and the Mariana trench [60]. Subsequent work at the Mariana trench showed that sheared serpentinites crop out all along the trench in a chain of seamounts. The exposure of these serpentinites is clearly associated with subduction processes and is thought to result from diapiric emplacement, either from material from the subducting plate [16] or from the mantle wedge [67]. One of these seamounts was drilling during ODP leg 125 [68].

This review paper concentrates on serpentinites collected at, and in the vicinity of mid-ocean ridges, i.e. where their formation is related to accretionary processes. The mechanisms responsible for the expo-

sure of serpentinites at the ocean floor in this context are discussed. A general description of typical ocean floor serpentinites is presented. The conditions of serpentinization (temperature, composition of the fluid phase) are evaluated. Our present knowledge of the consequences of serpentinization on the chemical composition of the crust, and on the physical properties of the ocean lithosphere is presented. Finally, the two major types of serpentinized peridotite hosted hydrothermal fields are described and their relation with serpentinization processes are discussed.

2. Occurrence of serpentinites at mid-ocean ridges

It is now well established that, in the global ridge system, serpentinites crop out essentially in slow to ultraslow spreading ridges [34]. In this environment, not only the amount of melting is low, but the lithosphere tends to be thicker. Melt delivery to the surface is episodic and tends to be focused at segment centres [49]. Moreover, the thick lithosphere allows tectonic activity and the development of deep rooted faults. Serpentinized peridotites are clearly not restricted to transform fault scarps, but also occur along the axial valley walls and even at the axial valley floor. A number of field studies suggests that, at least at segment ends, oceanic layer 3 may consist of more or less serpentinized peridotites intruded by gabbro pockets and directly overlain by basalts. This has been documented at the slow spreading Mid-Atlantic Ridge (MAR) [36, 71,81,88], at the ultraslow spreading South West Indian Ridge (SWIR) [8,49,97] and more recently at the slowest ridge of the global system, the Gakkel ridge in the Arctic [98]. A thick gabbro layer as well as a dike complex are often missing. At a Penrose conference in 1972 [110], combining seismic studies, results from seafloor dredging and observations in ophiolite complexes, a layered structure was proposed for the ocean lithosphere (Fig. 1). According to the Penrose model, beneath a sediment cover, the oceanic crust is composed of magmatic rocks. Layer 2 consists of basaltic rocks, either extruded on the seafloor as pillow-lavas or intruded as dikes. Layer 3 consists of gabbroic rocks crystallized at depth. The seismically defined MOHO, located at about 6 km beneath the seafloor, separates the crust from the underlying mantle (Layer 4) consisting in peridotites, residues of partial melting. The
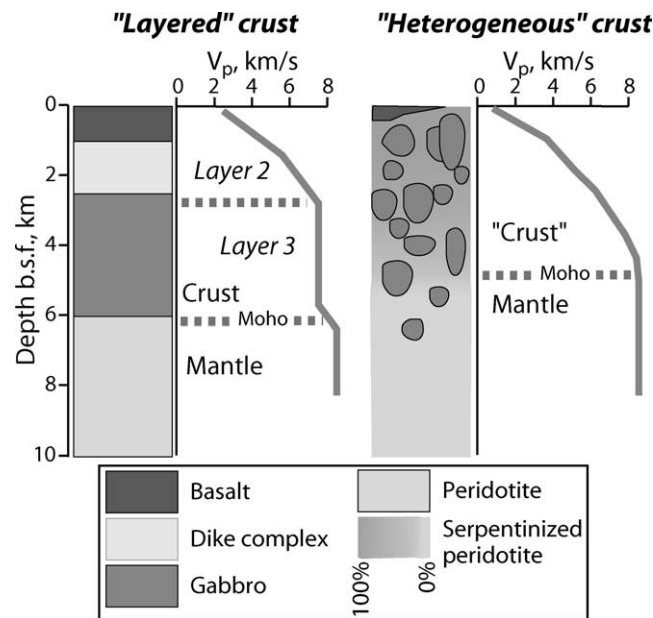
Fig. 1. Seismic velocity profiles and geological interpretation of a Penrose-type 'layered crust' [110] and a heterogeneous crust [34]. Note that the layered crust consists of magmatic rocks (basalts and gabbros) only, while the heterogeneous crust contains residual rocks (serpentinized peridotites).

Fig. 1. Profils de vitesses sismiques et interprétation géologique d'une croûte litée de type Penrose [110] et d'une croûte hétérogène [34]. La croûte litée est constituée uniquement de roches magmatiques (basaltes et gabbros), alors que la croûte hétérogène comprend des roches résiduelles (péridotites serpentinisées).
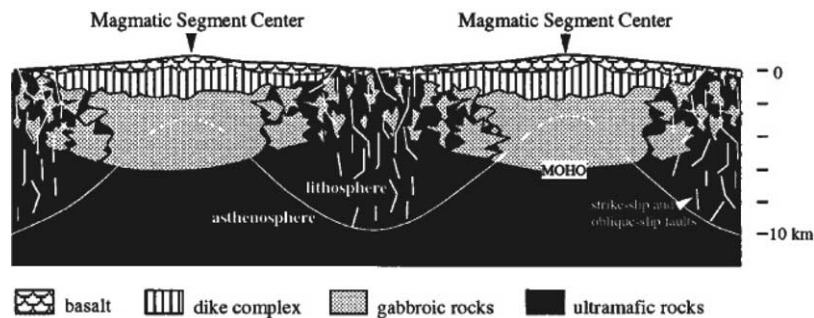

Fig. 2. Hypothetical along axis cross section of a slow-spreading ridge, from [36]. Based on geological observations at the Mid-Atlantic Ridge, this sketch suggests a different magma supply between the centre and the ends of the segments. At the centre, the crust is supposed to be layered and magmatic while its ends are heterogeneous, with small magma pockets enclosed in residual mantle-derived serpentinized peridotites.

Fig. 2. Coupe hypothétique le long de l'axe d'une dorsale lente, d'après [36]. Basé sur des observations géologiques à la dorsale médio-Atlantique, ce schéma suggère un apport magmatique différent entre le centre et les extrémités des segments. Au centre, la croûte est supposée litée et magmatique, alors qu'aux extrémités elle est hétérogène, constituée d'intrusions gabbroïques dans des péridotites résiduelles serpentinisées.

crust formed at a slow and ultraslow spreading ridge clearly does not fit the Penrose model. It does not have a layered structure but is heterogeneous and its architecture varies along its axis [36] (Fig. 2). The outcrop- ping of residual peridotites at segment ends is likely to result from the melt focusing at segment centres. In the absence or paucity of basaltic melt, plate divergence is accommodated by advection of asthenospheric man-

tle to the lithosphere and by tectonic processes that result in the exposure of rocks from the mantle. The tectonic activity also favours seawater penetration and alteration of the mantle peridotites. The layered and homogeneous seismic structure that is observed everywhere can be explained by the fact that gabbros and partially serpentinized peridotites have the same seismic velocities [34] (Fig. 1, see Section 6). This suggests that when serpentinized peridotites crop out at the surface, the MOHO does not correspond to the magmatic crust/residual peridotite boundary, but could be a hydration boundary, i.e. the boundary between serpentinized peridotites and fresh peridotites [73].

More recently, very low angle faults, i.e. megamullions or detachment faults, that accommodate spreading for long periods of time (i.e. over a million years), have been discovered at slow spreading ridges [33,91, 123,127]. These long lived faults expose large portions of the oceanic lithosphere, and serpentinites as well as talcschists commonly crop out on their surfaces.

This new perspective on accretionary processes at slow spreading ridges suggests that serpentinized peridotites make up a significant portion of the so-called oceanic 'crust' at slow to ultraslow spreading ridges, although at this stage, it is still difficult to quantify. On the basis of geological observations, Cannat et al. [36] tentatively suggest that exposure of serpentinites could represent 20% of the seafloor, but in volume they would not exceed 5–15% of the crust. On the basis of seismic data, Carlson [37] comes to the estimate of 5% maximum. Further work is undoubtedly needed for a better understanding.

By contrast, in fast spreading ridges, most evidence suggests that the crust is layered and consists of extrusive basalts, a dike complex and a massive gabbro layer overlying mantle peridotites (Fig. 1). In this case, the MOHO is interpreted as the transition between a magmatic crust and the residual mantle peridotites [117]. Peridotites occur only below the MOHO, i.e. at depths > 6 km. Given this general structure, major tectonic movements are necessary to expose them at the seafloor. Outcrops of serpentinized peridotites have been documented only in very particular areas: major transform faults (Garrett [14]), trenches opening at the boundary of rotating microplates, such as Easter and Juan Fernandez [46], and the tip of propagators such as Hess Deep [63]. In this case, as opposed to slow spreading environments, serpentinized

peridotites do not represent a significant portion of the crust. The presence of serpentinized ultramafics beneath the gabbro layer cannot be completely ruled out, but serpentinization must then occur off axis, when the temperature has dropped below 500 °C.

Sample suites of serpentinized peridotites from all these environments have led to various types of studies (mineralogy, petrology, geochemistry, physical properties). The most comprehensive data sets come from sites drilled by the Ocean Drilling Program (ODP). Two adjacent sites (670 and 920) are located at the Mid-Atlantic Ridge, in the western wall of the axial valley of the MARK area (23°N) and represent serpentinites from a slow spreading environment [35, 48]. Site 895 is located on the intrarift ridge of Hess Deep, which exposes rocks generated at the fast spreading East Pacific Rise [70]. The other samples which are referred to in this paper have been either dredged or collected with submersibles.

3. Mid-ocean ridge serpentinite textures and mineral assemblages

Abyssal peridotites collected from the seafloor consist primarily of harzbugites, with minor dunites and lherzolites. They are always between partly and completely altered. Altered peridotites display various appearances in colour: black, dark or light green, red, yellow. Serpentinites are generally black or green, while yellowish to reddish rock contain abundant clay minerals. This section concentrates on serpentinites sensu stricto, and synthesizes observations made on different sample sets [7,14,47,50,65,74,84,87,96,100, 101,111].

3.1. Textures

Serpentinization is always extensive. The extent of serpentinization, i.e. the percentage of secondary minerals, generally varies between 80 and 100%, but peridotites with as little as 50% serpentinization are occasionally found. Dunites are generally more heavily serpentinized than harzburgites. Most of the described serpentinites are undeformed, i.e. have been altered under static conditions: in hand specimen and under the microscope, primary textures are still identifiable (Fig. 3A). However, the samples are typically
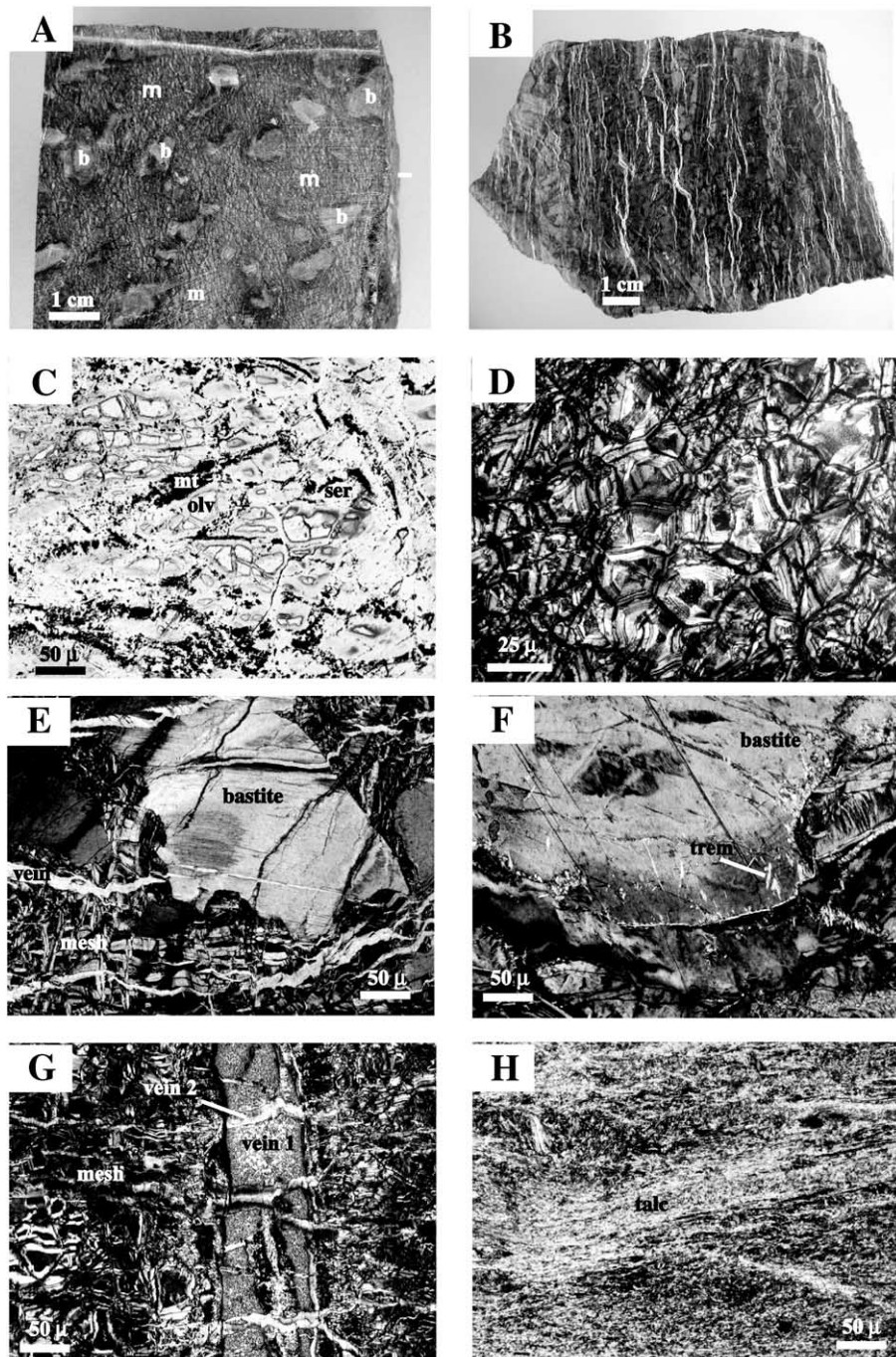
Fig. 3. Examples of serpentinite textures in hand specimen and photomicrographs. (**A**) Hand specimen of serpentinized peridotite. Serpentinization occurred under static conditions and preserved the primary textures. Areas of mesh texture (m) pseudomorphing olivine crystals are juxtaposed to bastites (b) pseudomorphing orthopyroxene crystals. Sample SDM DR34-1-1, M.A.R [36]. (**B**) Hand specimen of serpentinized peridotite. The sample is cross-cut by a dense network of parallel serpentine-filled veins. Sample EDUL DR23, SWIR [97].

cross-cut by vein networks, recording a complex history of fracturing, crack opening and fluid circulation [50,65]. The abundance and orientation of veins is very variable. A dense network of parallel veins may generate an apparent schistosity, even though the vein filling minerals have grown perpendicularly to the vein walls, clearly under static conditions (Fig. 3B). Scarce sheared veins have also been reported [111] and dredged blocks often display slickensides on their outer surfaces.

Although not as common, deformed serpentinites have also been described [7,28,100]. In general, dredge collections typically contain a few percent of serpentine schist fragments, even if those are generally not studied. Recently discovered detachment surfaces may also yield tremolite-talc-serpentine schists. Drill cores of one of these surfaces at 15°45N, off axis the MAR show that these schists make up the fault zone [91].

Serpentinite breccias have also been reported. A first type consists of serpentinite clasts cemented by a carbonate matrix (generally calcite or aragonite). These rocks are similar to what is called ophicalcite in ophiolites, and may have, at least partly, a hydrothermal origin [26,28]. A second type consists of indurated serpentinite fragments of sedimentary origin, often displaying graded bedding. These sedimentary serpentinites are likely emplaced by gravity sliding or slumping [28].

In undeformed oceanic serpentinites, microscopic textures are quite similar to those described in continental serpentinites (see review in [104]). A first detailed description of ophiolite and ocean floor serpentinite textures [111] has been confirmed by subsequent studies. The primary mineralogy of abyssal peridotites consists of olivine $\pm$ orthopyroxene (opx) $\pm$ clinopyroxene (cpx) $\pm$ spinel. Thin section observations display a different sensitivity to alteration for the primary phases. Resistance typically increases from olivine through orthopyroxene to clinopyroxene. High temperature of serpentinization (see Section 4) may however modify this general rule. Olivine is replaced by serpentine in mesh textures, while ortho- and clinopyroxenes are replaced by bastite. In the mesh texture, broken olivine fragments are replaced by concentric layers of serpentine aggregates associated with magnetite grains. A fresh olivine kernel might be preserved at the center (Fig. 3C and 3D). Alternatively, the centre may consist of brucite or carbonate. Bastite is made up of serpentine fibers which mimic the orthopyroxene shape (Fig. 3E). Because clinopyroxene is more resistant to alteration, clinopyroxene exsolution lamellae are often preserved in bastites replacing orthopyroxene [7]. Talc and/or amphibole may be associated with

Fig. 3. (**C**) Photomicrograph of a mesh texture replacing olivine in a serpentinized peridotite. Parallel nicols. Fresh olivine kernels (olv) are preserved in serpentine cells (ser) surrounded by magnetite layers (mt). Sample HS13-1, M.A.R [124]. (**D**) Photomicrograph of a mesh texture completely replacing olivine. Crossed nicols. Each cell of the mesh texture consists of concentric layers of serpentine. Sample ODP Leg 153, 920D 5R2 #12, M.A.R. [35]. (**E**) Photomicrograph showing a bastite replacing orthopyroxene isolated in serpentine in a mesh texture (pseudomorphs after olivine). Crossed nicols. Late veins cross-cut both the bastite and the mesh. Sample ODP Leg 153, 920D 3R2 #7, M.A.R. [35]. (**F**) Photomicrograph showing a bastite consisting of serpentine and minor tremolite fibers (trem). Crossed nicols. Sample HS13-7, M.A.R [124]. (**G**) Photomicrograph showing a serpentinite with a mesh texture cross-cut by two perpendicular sets of serpentine veins. Crossed nicols. Sample ODP Leg 153, 920D 7R2 #4, M.A.R. [35]. (**H**) Photomicrograph of a talc-serpentine schist. The primary texture is completely obliterated by recrystallization under deformation conditions. Crossed nicols. Sample BR28, pc3. M.A.R. [58].

Fig. 3. Exemples de textures de serpentinites en macro-échantillons et au microscope. (**A**) Echantillon de péridotite serpentinisée. La serpentinisation a eu lieu en régime statique et a préservé les textures primaires. Des zones à texture maillée (m) remplaçant les cristaux d'olivine sont juxtaposées à des bastites (b) remplaçant les orthopyroxènes. Echantillon SDM DR34-1-1, M.A.R [36]. (**B**) Echantillon de péridotite serpentinisée, recoupé par un dense réseau de veines parallèles remplies de serpentine. Echantillon EDUL DR23, SWIR [97]. (**C**) Photographie au microscope d'une texture maillée remplaçant l'olivine dans une péridotite serpentinisée. Nicols parallèles. Des coeurs d'olivine fraîche (olv) sont préservés dans des cellules de serpentine (ser) entourées de magnétite (mt). Echantillon HS13-1, M.A.R [124]. (**D**) Photographie au microscope d'une texture maillée remplaçant complètement l'olivine. Nicols croisés. Chaque cellule consiste en couches concentriques de serpentine. Echantillon ODP Leg 153, 920D 5R2 #12, M.A.R. [35]. (**E**) Photographie au microscope d'une bastite remplaçant un orthopyroxène isolé dans la serpentine maillée remplaçant l'olivine. Nicols croisés. Des veines tardives recoupent à la fois la serpentine maillée et la bastite. Echantillon ODP Leg 153, 920D 3R2 #7, M.A.R. [35]. (**F**) Photographie au microscope d'une bastite formée de serpentine et de fibres de trémolite (trem). Nicols croisés. Echantillon HS13-7, M.A.R [124]. (**G**) Photographie au microscope d'une serpentine à texture maillée, recoupée par deux générations de veines orientées perpendiculairement. Nicols croisés. Echantillon ODP Leg 153, 920D 7R2 #4, M.A.R. [35]. (**H**) Photographie au microscope d'un schiste à talc et serpentine. Nicols croisés. La texture originelle est complètement oblitérée par les recristallisations en régime de déformation. Echantillon BR28, pc3. M.A.R. [58].
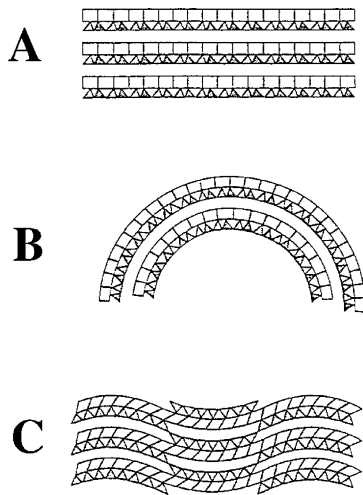
Fig. 4. Serpentine species crystallographic structures: A = lizardite; B = chrysotile; C = antigorite. Triangles represent 4-coordinated Si and more or less deformed squares represent 6-coordinated Mg (from B. Devouard, pers. comm.).

Fig. 4. Structures cristallographiques des espèces serpentineuses : A = lizardite ; B = chrysotile ; C = antigorite. Les triangles représentent des tétrahèdres de Si et les carrés plus ou moins déformés des octahèdres de Mg (B. Devouard, comm. pers.).

the alteration of orthopyroxene (Fig. 3F). In these statically altered rocks, it is generally easy to reconstruct the primary assemblages because the secondary minerals perfectly pseudomorph the original phases, even if cross-cutting veins are normally abundant (Fig. 3G) Some rocks, however, show evidence of recrystallization which may obliterate the primary textures [121].

In serpentine schists, the original texture has been completely modified by deformation and recrystallization (Fig. 3H). In talcschists, the ultramafic precursor can be inferred from the mineral assemblage (i.e. the presence of spinel grains), or from the bulk chemistry [58].

The fabrics of mid-ocean ridge serpentinites clearly demonstrate that most of the serpentinization occurs under static conditions, by reaction of the peridotite with a fluid phase driven through fractures and cracks. These undeformed textures are in agreement with a non-diapiric emplacement.

3.2. Mineralogy

Because the primary mineral assemblage of abyssal peridotites is relatively constant, the secondary assem-
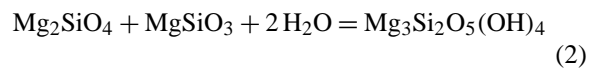
blage resulting from peridotite hydration is simple. A typical mid-ocean ridge serpentinite is made up of serpentine minerals + magnetite ± talc ± brucite ± tremolite. The most common accessory minerals consist of ferrit-chromite, chlorite, native metals and sulfides, clay minerals, diopside, secondary olivine, hornblende. Textural relationships, however, suggest that not all these phases are in equilibrium: they record phases that pre- or postdate the serpentinization event.

3.2.1. Serpentine minerals

A number of general reactions are often used to describe the formation of serpentine. In a purely magnesian system, the most commonly referred to are the following:

$$2\,Mg_2SiO_4 + 3\,H_2O = Mg_3Si_2O_5(OH)_4 + Mg(OH)_2 \tag{1}$$
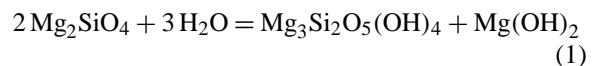
olivine + water = serpentine + brucite

$$Mg_2SiO_4 + MgSiO_3 + 2\,H_2O = Mg_3Si_2O_5(OH)_4 \tag{2}$$

olivine + orthopyroxene + water = serpentine

The serpentine species, however, may vary. Serpentine minerals are trioctahedral 1:1 layer silicates. They consist of alternating infinite sheets of 4-coordinated Si and 6-coordinated Mg. The three dominant species are lizardite, chrysotile and antigorite, which differ by their crystal structure. Lizardite consists of planar layers (Fig. 4A). Chrysotile consists of scrolled layers, which tend to form cylinders (Fig. 4B). In antigorite, the 1:1 layer periodically reverses, resulting in the loss of a octahedral coordinated sites (Fig. 4C). The three species can be distinguished by their XRD patterns; however, the crystal structures are best illustrated by TEM images (see review in [104,105]).

The general formula of serpentines is $Mg_5\{Si_2O_4\}$ $(OH)_4$. Substitution of Al and Fe^{3+} for Si may occur in tetrahedral sites, and that of Fe^{2+}, Fe^{3+}, Cr, Al, Ni and Mn for Mg in octahedral sites. It has been shown that lizardite tends to accept more substitution than chrysotile, and is typically more enriched in Al, although their compositions overlap [101,133]. Antigorite, however, because it lacks octahedral sites, is not strictly a polymorph. This results in the loss of Mg and $(OH)_4$ with respect to Si, and antigorite is therefore systematically enriched in silica [9,128,132].

All the serpentinites collected from the seafloor display lizardite as a dominant phase ([100,101,111] and references therein). It is found in the mesh texture as well as in the bastites. Chrysotile may be associated with lizardite. Chrysotile is the major phase occurring in veins. Antigorite has also been reported, but is definitely more scarce, associated with veins as well shear zones [100]. Recrystallizations generally result in the replacement of lizardite by chrysotile [121].

It is difficult to assess a specific composition to the different serpentine species in ocean floor serpentinites, as the serpentine variety is generally not determined when the chemical analyses are available. Moreover, the coexistence of lizardite and chrysotile in undetermined proportions is common in specific sites such as mesh after olivine or bastites. However, the microtextural site where the serpentine has crystallized clearly influences its chemistry [74,96]. Serpentine replacing olivine is typically devoid of aluminium and chromium but contains some nickel, matching the composition of olivine. By contrast, serpentine from bastites contains aluminium and chromium. The Mg# is not as consistent, because it may be controlled by external factors such as the oxygen fugacity which influences the Fe^{3+}/Fe^{2+} ratio; the amount of iron in serpentines varies with the abundance of associated magnetite, and therefore reflects oxidixing conditions [108]. When recrystallization occurs, the secondary serpentine is often chrysotile, replacing primary lizardite [121]. Its composition shows less substitution, as if recrystallisation resulted in serpentine minerals closer to the ideal formula. Serpentine in veins also tends to have less substitutions, which is consistent with the fact that Al, Cr, Ni are relatively immobile during alteration and therefore remain in their original microstructural site, and with the predominance of chrysotile.

3.2.2. Magnetite

Magnetite is ubiquitous in serpentinites and is the product of the serpentinization reaction of the iron end member. Incorporating iron, reaction (1) can be modified in the following way:

$$6\,(Mg, Fe)_2SiO_4 + 7\,H_2O$$
$$= 3(Mg, Fe)_3Si_2O_5(OH)_4 + Fe_3O_4 + H_2 \qquad (3)$$
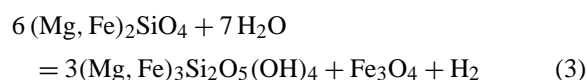
It is important to note that the oxidation of iron to form magnetite generates hydrogen (see Section 7). Mag-

netite often underlines the concentric layers of serpentine in the mesh texture. Its grain size is generally very small (in the order of a few microns or below), although occasionally euhedral crystals may reach over 10 μ (Fig. 3C).

3.2.3. Talc

Talc is commonly associated with the alteration of orthopyroxene. It generally occurs along cracks, progressively pseudomorphing the large crystals. It results from the following reaction:
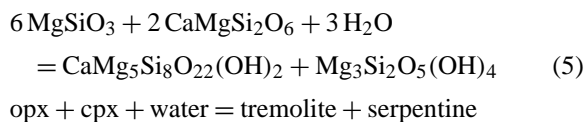
$$6\,MgSiO_3 + 3\,H_2O$$
$$= Mg_3Si_2O_5(OH)_4 + Mg_3Si_4O_{10}(OH)_2 \qquad (4)$$

orthopyroxene + water = serpentine + talc
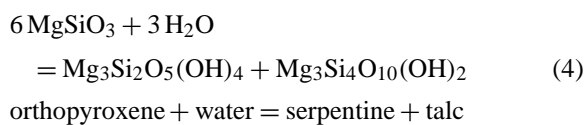
Talc is also present in deformed rocks, as a major constituent of serpentine-talc schists.

3.2.4. Amphiboles

Amphiboles often occur in serpentinites, although they are generally not very abundant.

The most common variety is tremolite. Texturally, it forms needles, generally associated with the alteration of pyroxenes (Fig. 3F). It may result from the following reaction (in a purely magnesian system):

$$6\,MgSiO_3 + 2\,CaMgSi_2O_6 + 3\,H_2O$$
$$= CaMg_5Si_8O_{22}(OH)_2 + Mg_3Si_2O_5(OH)_4 \qquad (5)$$

opx + cpx + water = tremolite + serpentine

Tremolite may contain some iron, as well as some aluminium and chromium.

Other types of amphiboles have also been described, although less frequently. In particular, magnesio-hornblende, edenitic hornblende, cummingtonite have been identified in serpentinites. However textural relationships suggest that they predate the serpentinization event [14,84].

3.2.5. Brucite

Brucite is an Mg-hydroxide which is only occasionally found in oceanic serpentinites. At Hess Deep, however, it occurs as a major phase [65,96]. Its ideal formula is $Mg(OH)_2$, but an Mg is often substituted by Fe^{2+}. It occurs either in the core of mesh texture, or more often in veins. Its formation is generally described by reaction (1).

3.2.6. Other minerals

Ferrit-chromite results from the alteration of aluminous spinel. This reaction provides aluminium, and a rim of chlorite is generally present around the altered spinel grains [74]. Secondary sulfides (pentlandite, marcasite, haezlewoodite, etc.) and native metals and/or alloys (native Cu, arawuite, taenite) have also been described [4]. They are inferred to result from the recrystallization of primary sulfides during serpentinization. Carbonates occur essentially in veins and as breccia matrix, and are generally aragonite and calcite. They correspond to very late stages and are not in equilibrium with the serpentine minerals.

3.2.7. Conclusions

This review of the mineral assemblages in serpentinites from mid-ocean ridges points out the predominance of lizardite and minor chrysotile, associated with magnetite. Other phases are much less abundant and are associated with particular mineral domains. It also suggests that the chemistry of serpentine species is largely controlled by the microstructural site. It should be pointed out that the presence of primary mineral relics, the juxtaposition of primary mineral pseudomorphs and the occurrence of cross-cutting vein networks are not in favour of equilibrium at the sample scale.

4. Conditions of serpentinization

The serpentinization of abyssal peridotites results from their interaction with large volumes of a hydrous fluid, at temperatures below 500 °C, maximum stability of serpentine minerals [32], although a number of studies suggests that seawater penetration in the peridotites may start at a higher temperature [14,84].

Although the serpentinites are presently exposed on the seafloor, a number of factors indicate that at least part of the serpentinization occurred at depth, when the peridotites were cooling down. In this section, the conditions of serpentinization, i.e. the pressure, temperature, oxygen fugacity as well as the nature and composition of the fluid phase will be discussed. It is important to keep in mind that serpentinites are polyphased rocks that record successive stages of crystallization. This section will essentially consider processes associated with the peak of crystallization, i.e. the replacement of olivine by the mesh textured serpentine and replacement of pyroxenes by bastite. Determining the temperature and pressure of serpentinization is not an easy task, because serpentine minerals are stable over a wide range of temperatures (between 500 °C and room temperature) and because reaction producing serpentines are relatively insensitive to pressure.

4.1. Pressure of serpentinization

The maximum pressure at which serpentinisation occurs is reasonably well constrained by the geodynamic setting. The depth of MOHO generally does not exceed 6 km. It may attain a maximum of 10 km and can be shallower at slow spreading ridges (< 3 km occasionally). High seismic velocities beneath the MOHO indicate that the mantle is composed of fresh peridotites. Therefore, serpentinites form at a maximum depth of 10 km but more generally at 6 km and even less when the MOHO is shallower. This translates into a maximum pressure in the order of 3 kb, and more generally < 2 kb, quite low compared to orogenic belts. Precise indicators, unfortunately, are lacking, to better constrain the pressure, and therefore the actual depth of serpentinization within the lithosphere.

4.2. Temperature of serpentinization

To estimate the temperature, a number of indicators can be used, but their precision remains poor, as will be discussed. Not only the stability field of serpentine minerals is not well constrained, but also the attainment of equilibrium is not really demonstrated. Finally, as evidenced by the numerous generations of veins, serpentinization does not occur in a single event.

4.2.1. Stability of serpentine species

Based on experimental work, the general consensus is that chrysotile and lizardite are stable at temperatures lower than antigorite [59,101]. The first phase diagram of serpentine species was constructed by Evans [59], based on experimental work. It showed that forsterite can be stable down to 400 °C, and that antigorite is the serpentine species stable at high temperatures (up to 500 °C). This phase diagram is consistent with his field observation in the central
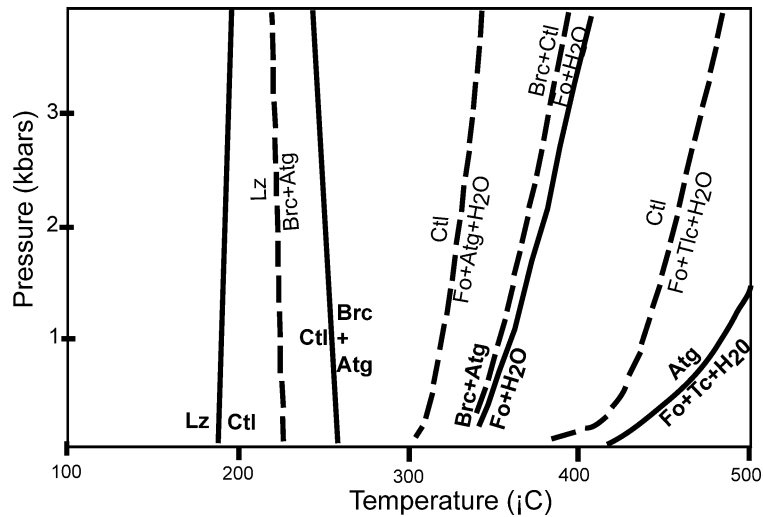
Fig. 5. Phase relationships of serpentine species and related minerals in a temperature–pressure diagram. Simplified from [104]. Continuous lines represent stable reaction curves, dashed lines, metastable reaction curves. Atg = antigorite; Brc = brucite; Ctl = chrysotile; Fo = forsterite; Lz = lizardite; Tc = talc.

Fig. 5. Relations de phase des espèces serpentineuses et minéraux associés dans un diagramme pression–température. Simplifié de [104]. Les lignes continues représentent les courbes de réaction stables, les lignes tiretées les courbes de réaction métastables. Atg = antigorite ; Brc = brucite ; Ctl = chrysotile ; Fo = forstérite ; Lz = lizardite ; Tc = talc.

Alps. An independent calculation of the temperature for the serpentine species was made using $\delta^{18}O$ (see below). The formation temperature for antigorite, chrysotile and lizardite were estimated at 235, 180 and 125 °C, respectively [129]. More recently, a more precise phase diagram was constructed on the basis of thermodynamic data [104] and shows the sequence antigorite>chrysotile>lizardite with decreasing temperature (Fig. 5). It also shows that forsterite is stable down to 350 °C.

In ocean floor serpentinites, reactions are retrograde (progressive hydration of a cooling peridotite), as opposed to the western Alps serpentinite section [59]. The peak of serpentinization is characterized by a predominance of lizardite ± minor chrysotile. Antigorite is extremely scarce. This would suggest relatively low temperatures ($\ll 200$ °C). Other indicators, such as associated minerals and ^{18}O fractionation, disagree with this estimate and suggest high temperatures (> 300 °C) (see below). Moreover, the experimental reaction between peridotite and seawater at 300 °C and 500 bars produced lizardite as a major phase [114]. This discrepancy again raises the question of equilibrium attainment in oceanic serpentinites. Another possible explanation for the widespread oc-

currence of lizardite is its ability to depart from the ideal formula by incorporating Fe^{2+}, Fe^{3+} and Al. Some authors have shown that these substitutions enlarge the stability field towards higher temperatures [38,94,106]. Crystallization of lizardite in olivine and pyroxene could also be structurally controlled by the preexisting phases. In any case, it is obvious that the nature of the serpentine species remains a poor indicator of the temperature for oceanic serpentinites.

4.2.2. Mineral assemblages of serpentinites

Besides serpentine minerals, other phases occur in serpentinites or associated cross-cutting dikelets and provide some constraints on the temperature.

The significance of talc in serpentinites has been largely debated because talc is stable over a wide range of temperatures. It does not seem to be a good temperature indicator because its formation is controlled by other factors, particularly by silica activity in the fluid phase [74]. This is confirmed by the experimental reaction between peridotites and seawater at 300 °C which shows that talc formation is favoured by high activities of SiO_2, MgO and H^+ [78]. Further experiments at 400 °C [3] suggest that at high temperatures, the preferential alteration of pyroxenes (with respect

to olivine) results in fluids enriched in dissolved Ca, SiO_2, Fe and H^+ which favour the formation of Si-rich silicates (talc and tremolite). These results are in agreement with the observed association of talc with pyroxenes. The presence of talc would therefore indicate higher temperatures of serpentinization, as well as high silica activity.

The common presence of chlorite and tremolite suggest temperatures consistent with greenschist facies conditions, i.e. in the range of 300–500 °C. For example, in serpentinites at Hess Deep [65,96] as well as Garrett Fracture zone [14], the association with altered gabbros dikes or impregnations containing chlorite, albite, actinolite as secondary phases suggest temperature conditions between 300 and 500 °C. Minor phases may also be informative. In Hess Deep serpentinites, the presence of a FeNi-alloy, taenite even suggests temperatures as high as 450 °C [72]. Another indication of temperature is given by the respective dissolution rates of olivine and orthopyroxene. Experimental reactions have shown that olivine is preferentially dissolved at temperatures around 250–300 °C, while orthopyroxene is rapidly dissolved at temperatures above 400 °C [93]. If all the orthopyroxene has been serpentinized in a given sample, while olivine relicts are still present, this indicates reactions at high temperature (> 400 °C). This case has been reported in samples from Hess Deep [121].

4.2.3. Oxygen isotopes

^{18}O fractionation also allows us to estimate serpentine crystallization temperatures. The starting material is a peridotite with a well defined mantle value ($\delta^{18}O$ = 5–6‰). The reacting fluid phase is inferred to be seawater ($\delta^{18}O$ = 0). Empirical fractionation curves between serpentine and water as well as serpentine and magnetite have been proposed [129,130] and recently refined [65]. However, because these curves have not been experimentally constrained, the uncertainty on temperature estimates remain very high, up to 50–120 °C [2,65]. A first result is to show that the fractionation between serpentine and water depends on the temperature: the $\delta^{18}O$ of the serpentine is heavier than the starting material at low temperatures, lighter at high temperatures, the critical change appears around 100–200 °C. Fig. 6 shows a compilation of $\delta^{18}O$ measured in mid-ocean ridge serpentinites. It shows a large dispersion in the values, between 0 and +12‰, en-

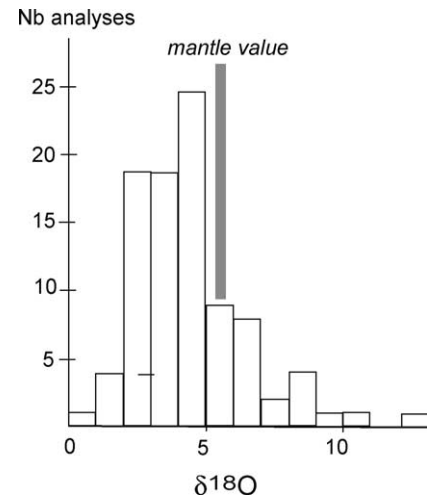Fig. 6. Compilation of $\delta^{18}O$ measurements in serpentinites and serpentine minerals from mid-ocean ridge environments. The values span a wide range, with a peak at +3 to +5‰. Data from: [1,2,30, 47,65,87,129,130].

Fig. 6. Compilation des données de $\delta^{18}O$ dans les serpentinites et minéraux serpentineux des environnements de dorsales océaniques. Données de [1,2,30,47,65,87,129,130].

closing the mantle value. This suggests that serpentinization reactions occur over a wide range of temperature. The $\delta^{18}O$ is also influenced by the water/rock ratio (W/R). The minimum W/R required to convert fresh peridotites to serpentinites stoichiometrically is 0.13 [113]. As a rule, at higher W/R, isotopic compositions are more strongly modified [113]. For the MARK area serpentinites, a W/R in the range of 0.55 to 1 has been calculated at 400 °C [2], depending on the fluid composition.

More precise temperatures can be tentatively evaluated. The serpentine/water fractionation curve [129] allows the calculation of the temperature if the $\delta^{18}O$ of the fluid phase is constrained. It is reasonable to assume that seawater is the major component of the reacting fluid phase. However, as it penetrates into the crust, it reacts to form secondary minerals and its $\delta^{18}O$ is consequently modified. An obvious example of this compositional evolution of the reacting fluid phase is the $\delta^{18}O$ of fluids venting at black smokers. These fluids, which are the end product of seawater convecting cells in the crust, yield systematic positive $\delta^{18}O$ values, intermediate between seawater ($\delta^{18}O$ = 0) and the magmatic rocks ($\delta^{18}O$ = 5–6) with which it has reacted – see the review in [115]. For instance, at the

Table 1
Temperature estimates for serpentine formation from oxygen isotopes

Tableau 1
Estimations de température des conditions de serpentinisation à partir des compositions isotopiques de l'oxygène

Location	Reference	Temperatures	Indicator
MAR 1°N and 43°N	[130]	118° (lizardite) 180° (chrysotile) 235° (antigorite)	$\delta^{18}O$ fractionation between serpentine and magnetite
Vema and Romanche FZ, MAR	[30]	30–177 °C (1) 45–233 °C (2)	$\delta^{18}O$ fractionation between serpentine and fluid reacting fluid = (1) seawater, $\delta^{18}O = 0$; (2) hydrothermal fluid, $\delta^{18}O = 1.6‰$
ODP Site 670 MARK	[87]	113–246° (1) 160–385 °C (2)	$\delta^{18}O$ fractionation between serpentine and fluid reacting fluid = (1) seawater, $\delta^{18}O = 0$; (2) hydrothermal fluid, $\delta^{18}O = 2.4‰$
ODP site 920, MARK	[2]	430–590 ±120 °C	$\delta^{18}O$ fractionation between serpentine and magnetite
EPR Hess Deep	[1]	325 ± 50 °C 55–135 (1) 80–190 115–285 (3)	$\delta^{18}O$ fractionation between serpentine and magnetite $\delta^{18}O$ fractionation between serpentine and fluid reacting fluid = (1) seawater, $\delta^{18}O = 0$; (2) hydrothermal fluid, $\delta^{18}O = 2‰$ (3) hydrothermal fluid, $\delta^{18}O = 4‰$
ODP Site 895 Hess Deep	[65]	297–386 ± 50 °C 410–533 ± 50 °C	$\delta^{18}O$ fractionation between serpentine and magnetite
SWIR 52–69°E	[47]	116–275 ° (1) 160–427° (2)	$\delta^{18}O$ fractionation between serpentine and fluid reacting fluid = (1) seawater, $\delta^{18}O = 0$; (2) hydrothermal fluid, $\delta^{18}O = 2.4‰$

Snake Pit vents on the Mid-Atlantic Ridge, hydrothermal fluids yield a $\delta^{18}O$ of 2.30 [80]. The composition of fluids involved in serpentinization reactions remains unknown, but is likely to have evolved with respect to seawater. In the absence of a precise composition for the fluid phase, a number of authors have used different $\delta^{18}O$ values varying between 0 (pure seawater) and 4 (evolved seawater), and calculated a temperature range. Table 1 summarizes the temperatures obtained and shows a wide spectrum, ranging from 30 °C to over 400 °C.

Calculations based on empirical oxygen isotope fractionation curve between serpentine and magnetite [65,129] help avoid assumptions on the composition of the fluid phase. Equilibrium temperatures have been calculated for only a few examples, because separating magnetite from serpentine is not often possible due to the very small grain size of magnetite. The results are again very variable (Table 1) and reach up to 500 °C.

In conclusion, despite the uncertainties in the temperature estimates due to the lack of experimental calibration as well as the fact that equilibrium attainment may not be reached, this review clearly demonstrates that serpentinization starts at a high temperature, in the range of 300–500 °C, but temperatures in the range

of 100 °C are also reported (see Table 1 and references therein). It is interesting to point out that samples yielding the highest temperature come from drill holes (MARK, Hess Deep). The other samples, collected from the seafloor, and often off axis in fracture zone, may have been subjected to later re-equilibration at or near the seafloor.

4.3. Nature and composition of the altering fluid phase

An ocean floor serpentinite typically contains 10–15% of water or even higher, depending on the extent of serpentinization. The formation of serpentinites from an essentially anhydrous peridotite certainly heavily involves seawater. However, as already pointed out, some tracers suggest that the fluid may have evolved from pure seawater by reaction with the ocean crust and/or mixing with other fluids.

Stable isotopes are good tracers for the nature of the altering fluid. The $\delta^{18}O$ values measured in serpentinites suggest that the fluid phase has a $\delta^{18}O \ll 5.5‰$, the average value of fresh peridotites and consistent with dominant seawater. As discussed above, as seawater penetrates into the crust, however, it re-

acts with the rocks and its composition evolves. This evolution results in heavier $\delta^{18}O$. A possible way of estimating the $\delta^{18}O$ of the fluid phase is to constrain the temperature using the fractionation between serpentine and magnetite, and then calculate the composition of the fluid phase using the partition coefficient between serpentine and fluid at a given temperature. At MARK (ODP Site 920), the calculated range of $\delta^{18}O$ for the fluid phase varies between 3.3 and 4.4‰ at 350 °C, and between 4.3 and 5.4‰ at 450 °C. At Hess Deep, consistent values of 4‰ for a temperature of 325 °C have been calculated for a sample collected by submersible [1], and 3.3–4.4‰ at 450 °C for the drilled samples [65]. Even with the uncertainty, it can be stated that $\delta^{18}O$ suggests evolved seawater rather than unaltered seawater. The relatively heavy value of 6.6‰ found at Hess Deep could result from mixing with magmatic fluid [65].

A possible mixing of unaltered seawater with a fluid of deep origin has also been suggested from δD values. Ocean floor serpentinites are characterized by very light δD (< -60‰), which cannot be explained by simple interaction with interaction with seawater, and their origin has been debated [65,116,130]. The mixing with magmatic or metamorphic fluids (resulting from dehydration reaction of previously altered ocean crust) has been invoked [116,130]. However, at Hess Deep, at least 20% of magmatic fluid is required to explain the very light δD values. Given the very low water content of MORB magmas, this percentage does not seem realistic. Moreover, there is no petrological evidence for intensive dehydration reactions. An alter-

native explanation could be the D/H fractionation during the production of molecular hydrogen associated with serpentinization [65].

At Hess Deep, the existence of a magmatic component is also suggested by $\delta^{13}C$ signatures [65]. The thermal decomposition of the serpentinites produces CO_2 with a $\delta^{13}C$ consistent with magmatic values (-4.5–7.8‰), as opposed to aragonite veins which are consistent with oceanic carbon.

A very low oxygen fugacity during serpentinization can be inferred from the presence of sulfides and metal alloys [64,101]. In Hess Deep serpentinites, the paragenesis of opaque phases consisting of magnetite + awaruite + pentlandite $\pm$ heazlewoodite, stable at temperatures ranging from 400 to 100 °C, indicates highly reducing conditions and low $f O_2$ [4]. These extreme conditions are attributed to the production of H^+ during silicate reactions (see reaction (3)) which maintains low $f O_2$ and produces H_2S from primary sulfides.

Strontium isotopes are also a good tracer for the interaction with seawater. A number of studies have shown that the $^{87}Sr/^{86}Sr$ span a range between mantle (0.7023) and present-day seawater (0.7092) values with a peak around 0.708–0.709, therefore arguing for a seawater dominated fluid phase (Fig. 7). The large interval is interpreted in terms of the mixing of three components: MORB, mantle peridotites and seawater [85]. MORBs and oceanic peridotites have similar strontium isotopic compositions, but the concentration is much higher in MORBs than in peridotites [85]. MORBs and peridotite have the same strontium
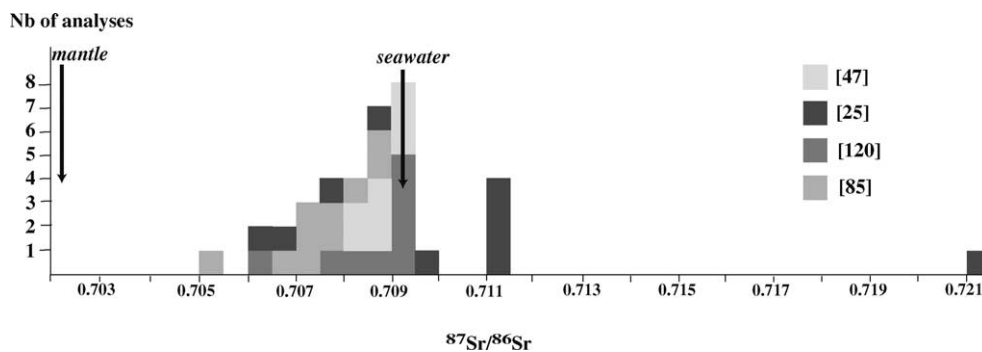
Fig. 7. Compilation of $^{87}Sr/^{86}Sr$ ratios in serpentinites and serpentine minerals from mid-ocean ridge environments. Data from [25,47,85,120]. The data from [118] are not shown because they correspond to magnetic fraction separates.

Fig. 7. Compilation des rapports $^{87}Sr/^{86}Sr$ dans les serpentinites et minéraux serpentineux des environnements de dorsales océaniques. Données de [25,47,85,120]. Les données de [118] ne sont pas figurées, car elles correspondent à la fraction magnétique.

isotopic compositions, but their strontium concentrations vary from above 100 ppm in basalts to less than 10 ppm in peridotites. Because the strontium content of peridotites is very low compared with seawater, interaction with seawater is dominated by the $^{87}Sr/^{86}Sr$ ratio of the fluid, and serpentinites should rapidly be in equilibrium with seawater, depending on the water/rock ratio. Intermediate values may result either from low water/rock ratios, or from interaction with the overlying basaltic crust during penetration at depth. Fig. 7 also points out that some whole rock analyses of serpentinites yield puzzling $^{87}Sr/^{86}Sr$ ratios, higher than seawater. These values were first documented for serpentinized peridotites from the equatorial M.A.R. [25]. The proposed explanation for these values was that the peridotites were remnants of continental mantle left behind during the breakup of Pangea [24]. More recently, such high $^{87}Sr/^{86}Sr$ ratios were found again in serpentinized abyssal peridotites from other localities [118]. On the basis of mineral separates and leaching experiments, these authors argue that the high ratios are due to detrital sediment particles of continental origin infiltrated through the cracks of the serpentinites. Although this process is not related to serpentinization, it should be kept in mind because it may affect the $^{87}Sr/^{86}Sr$ ratios of abyssal serpentinites.

The combined use of stable and radiogenic isotopes as tracers leads to the conclusion that the fluid phase involved in the serpentinization reaction at mid-ocean ridges consists of evolved seawater, with a possible minor magmatic component.

5. Elemental fluxes during serpentinisation

The first and major consequence of serpentinization is hydration. Serpentine minerals contain over 12% water. In serpentinites, they represent the major phase and the amount of water has often been used as a proxy for the degree of serpentinization. The second consequence is oxidation of iron due to the formation of magnetite by reaction (3). However, there has been a number of debates on whether, besides these two effects, serpentinization has a chemical consequence on the bulk chemistry of the rocks. A good summary of these debates is given by O'Hanley [104]. The essence of the problem is the question of volume, because serpentinite has a much lower density than a fresh peri-

dotite (2.5 g/cm^3 versus 3.3 g/cm^3). If serpentinization occurs at constant volume, the decrease in density must be accompanied by a loss of chemical elements. By contrast, if the chemical elements remain constant, then there must be a volume increase to account for the decrease in density.

The problem of volume increase due to hydration has not yet been completely solved. Most ocean floor serpentinites have been formed under static conditions; serpentine pseudomorphing primary minerals preserve the details of the original texture, and does not favour a volume increase at the crystal scale. At the sample scale, however, vein networks are commonly reported and can account for a volume expansion. From observations in continental serpentinites, O'Hanley [103] proposes that progressive serpentinization produces a kernel pattern than can account for volume expansion. This model could apply to oceanic serpentinites, but, unfortunately, no such detailed outcrop observations are available.

The problem in evaluating chemical fluxes is that the fresh protolith is never available for comparison with the altered rock. Although peridotites are relatively homogeneous in terms of mineral assemblages, the mineral compositions may vary widely, reflecting the amount of melting as well as possible reaction with percolating melts. Therefore there is no 'standard composition' that could be used as a reference.

5.1. Major elements

On the basis of correlated variations between elements (CaO, Al$_2$O$_3$, FeO*/MgO) that can be interpreted in terms of primary processes, it has been suggested that most of the chemical variations among samples are due to the primary heterogeneity of the peridotites, even though some mobilization during serpentinization may also occur (i.e. loss of CaO) [100]. A more quantitative attempt to evaluate chemical fluxes was made in serpentinized peridotites from the Franciscan formation [45]. In this example, serpentinization, besides hydration, does not seem to affect major element concentrations, except for calcium. The consequence is a calculated volume increase of 35% for harzbugites and 48% for dunites. A study of serpentinized dunites and wehrlites from the Bay of Island ophiolites comes to the same conclusion [86]. On the basis of modal reconstructions, a volume increase

of 32% is estimated and mass balance calculation indicated evidence for appreciable metasomatism for CaO, Al_2O_3, FeO and MgO. No mass balance calculations have been attempted on serpentinized abyssal peridotites but the general consensus is that the major elements are not severely affected, which implies an overall volume increase [74,87,96]. The fact that serpentine minerals pseudomorphing primary phases commonly retain the minor elements such as Al, Cr and Ni is also in favour of immobility during serpentinization. The only evidence for a loss in magnesium has been documented in peridotites altered at low-temperature and is likely to be related to the formation of clay minerals [119]. In this case, an average of 5% MgO loss is estimated as a result of weathering (temperature $\ll 100\,°C$), probably when the rocks are exposed on the seafloor.

Experimental reactions between peridotite and water have been conducted at temperatures between 200 and 400 °C and a pressure of 500 bars, with the aim of constraining chemical fluxes [3,78,114]. The results remain inconclusive on the final chemical budget because equilibrium is not reached, but they help us to understand reaction pathways. In most experiments, SiO_2 initially increases in the solution while MgO and pH decrease. The low pH favours the dissolution of Fe, Mn, Zn. Subsequently, the pH increases and the dissolution rates decrease. The data show that reaction pathways are dependant on the mineral assemblages of the peridotites, the solution chemistry, in particular the MgO concentration which affects the pH, and therefore the dissolution of minerals and the water/rock ratios.

There is evidence for local metasomatism associated with serpentinization. The occurrence of rodingites, gabbroic dikes recrystallized to secondary assemblages rich in calsilicates (hydrogrossular, prehnite, epidote, pumpellyite), implies the input of calcium, generally considered to have been leached from the peridotites during serpentinization [7,14,76]. At Hess Deep, however, it has been argued that the incipient formation of rodingites could simply reflect a redistribution of sodium and calcium within the gabbroic bodies during the serpentinization event [96]. The other evidence for mass transfers during serpentinization is the presence of tremolite-talc schists often associated with serpentinites [58,66,91]. Pyroxene is serpentinized at temperatures as high as 500 °C, while

olivine is stable down to 400 °C. Serpentinization of pyroxenes definitely results in a loss of silica. An increased silica activity in the fluid results in the stability of talc and tremolite over serpentine [3]. If silica rich fluids are channelled in fault zones, the alteration of peridotites occurs under dynamic conditions and results in the formation of serpentine-talc-tremolite schists. However, this evidence for metasomatism remains volumetrically small compared with the bulk of massive serpentinites.

5.2. Trace elements

The behaviour of trace elements during serpentinization is not well constrained yet.

Serpentines are enriched in *chlorine*. In situ analyses of individual serpentine crystals document values between 90 and 14 800 ppm [74,84,96], see review in [6], with an average value of 1850 ppm. Bulk rock analyses confirm these numbers: 1065–1470 ppm in serpentinites from the 15°N detachment surface at the M.A.R. (Mével, unpublished data) and 168–2211 ppm in serpentinites from the SWIR (Decitre, unpublished data). Anselmi et al. [6] favour the location of Cl as isomorphic substitution for $(OH)^-$ groups in serpentines as opposed to secondary formed hydroxichloride. Früh-Green et al. [65] also report 6% chlorine in brucite veins, but brucite is not a common phase, except at Hess Deep. Further work is certainly necessary to better constrain which mineral partitions chlorine, but in any case, serpentinites are clearly a sink for chlorine.

Serpentinites are enriched in *boron* (100 ppm) compared with fresh peridotites (15–25 ppm) [125]. Values ranging from 24 to 110 ppm (corrected for the percentage of serpentinization) have subsequently been measured [30] on another suite of samples, also documenting an inverse correlation between B and temperature. The uptake of B is favoured at low temperatures ($< 50\,°C$). This behaviour was confirmed by experiments [114] which show that at 300 °C, there is no change in the B concentration of the reacting fluid, while it drastically decreases during cooling to 25 °C, suggesting that the boron uptake occurs during retrograde reactions with seawater.

Fluorine also seems to be taken-up during serpentinization. A bulk rock value of 204 ppm [122] of fluo-

rine is confirmed by in situ nuclear microprobe analyses [107] which yield an average of 206 ppm.

Decitre et al. [47] report bulk rock serpentinite concentrations for *lithium* ranging from 0.6 to 8.2 ppm, while the mantle value is 1–3 ppm. They conclude that serpentinized peridotites can be only a minor sink for Li. The δ^6Li suggest that Li is recycled from the altered ocean crust rather than seawater.

The behaviour of *sulfur* during serpentinization has been studied at Hess Deep in comparison with the Iberian margin [4]. At Hess Deep, high temperature serpentinization results in an slight uptake of sulfur (mean = 355 ppm versus 250 ppm for the mantle value). It reflects the combined effect of a decrease in sulfide sulfur (trace to 165 ppm) due to the breakdown of primary sulfides (replaced by metal alloys and sulfide phases containing less S) and an increase in sulfate sulfur (50 to 790 ppm) due to the uptake of sulfate from seawater. It is suggested that the wide spectrum of δ^{34}S (21‰ to −3.3‰) for sulfates reflects a mixing of seawater sulfates (high values) with sulfates derived from oxidation of sulfides. The δ^{34}S of sulfides varies from 1.5‰ to −23.7‰. The highest values are consistent with magmatic values, while the lowest are best explained by the microbial reduction of seawater sulfates during the late stage of serpentinization (at temperature < 120 °C). The combination of these processes results in a net increase in δ^{34}S (mean = 8‰) for bulk serpentinites. This study also indicates a difference with the Iberian margin serpentinites, formed at lower temperatures and higher fluid fluxes, where a higher microbial activity results in a higher uptake of total sulfur (mean S content = 3800 ppm) and a decrease in δ^{34}S (mean = −5‰). A subsequent study of MARK area serpentinites also documents high sulfur contents (up to 1 wt%) and high δ^{34}S in sulfides (3.7 to 12.7‰) [5]. In this case, however, the authors ascribe the enrichment in sulfur to a multistage reaction process. Aqueous fluids enriched in sulfur through hydrothermal reactions with subjacent gabbroic intrusions at temperatures in the range of 350–400 °C are subsequently involved in serpentinization reactions at temperatures < 300 °C. In any case, serpentinization obviously influences the global cycle of sulfur and results in a net increase of sulfur and a modification in the δ^{34}S.

The behaviour of *REE* as well as *radiogenic isotopes* during serpentinization is a major issue for petrologists because it is important to determine whether they retain their primary values; however, no systematic studies have been conducted on oceanic serpentinites. A review of studies on continental/ophiolitic peridotites [95] shows that there is no consensus on the behaviour of REE. The authors conducted experiments to better constrain this behaviour, by reacting a lherzolite, a harzburgite and a dunite with seawater at 300 °C. Again, the results remain ambiguous. For lherzolite and dunite, the REE remain immobile, while for the harzburgite, an uptake in LREE (La > Ce > Nd) occurs. The authors attribute this difference to the role of secondary Ca-bearing phases. It should be pointed out that some of the experiments produce anhydrite which is never observed in natural serpentinites because it has likely been redissolved by seawater at temperatures < 150 °C. These experiments also constrain the behaviour of some radiogenic isotopes, ^{143}Nd/^{144}Nd and ^{87}Sr/^{86}Sr. As discussed in Section 4, the ^{87}Sr/^{86}Sr ratio is strongly affected during serpentinization. But a ^{87}Sr/^{86}Sr versus ^{143}Nd/^{144}Nd binary diagram shows that, by contrast, neodymium isotopes are little affected. The representative points form a horizontal array at constant ^{143}Nd/^{144}Nd values of 0.51310–0.51314, consistent with mantle values. Only at very water/rock ratios could the ^{143}Nd/^{144}Nd ratio be also affected [119].

5.3. Discussion

This review shows that the chemical consequences of serpentinization are still not very well understood. It seems that serpentinization does not occur at constant volume and that major elements, besides hydration and oxidation, are not severely affected. Local metasomatism may result in the formation of rodingites and/or talc and tremolite schists. Serpentinites are clearly a sink for Cl, B, F and S. The behaviour of REE and some radiogenic elements seems to be dependent on the water/rock ratio, on the extent of serpentinization, and on the behaviour of pyroxene, since this phase concentrates most of these elements. Further work is clearly necessary to better understand the chemical fluxes associated with serpentinization processes. Now that it is recognized that serpentinites are a important component of the crust, it becomes crucial to constrain these fluxes. They may have a global impact on the composition of seawater. On the

other hand, when heterogenous oceanic lithosphere is entrained in subduction zones, there is a potential for recycling chemical elements into the mantle.

6. Consequences of serpentinization on physical properties of peridotites

Due to massive hydration and crystallization of secondary phases, the physical properties of abyssal peridotites are strongly modified by serpentinization. A summary of the major consequences are given in this section.

The average *density* of a fresh peridotite is approximately 3.3 g/cm^3. Serpentine minerals have a density of approximately 2.5 g/cm^3. Serpentinization is therefore responsible for a strong decrease in density. A compilation of density measurements of serpentinites [99] shows that, as expected, there is an inverse correlation between density and the extent of serpentinization (Fig. 8A). As discussed in Section 5, serpentinization does not seem to be accompanied by major chemical fluxes, and the consequence is an increase of volume. In the extensional environment of a mid-ocean ridge, this volume increase is likely accommodated by tectonic activity, as evidenced by vein networks.

The decrease in density affects the *seismic velocities*. Following the pioneer work of Christensen [43,

44], all the seismic velocities measured on serpentinites have shown a strong dependence with the degree of serpentinization. A compilation [99] shows an inverse relation between the amount of serpentinization and seismic velocities (Fig. 8B). A partially serpentinized peridotite may therefore have the same seismic velocities as a gabbro [37,77], and a seismically layered oceanic crust may be compositionally heterogeneous (Fig. 1) [34]. Because observations and sampling on the seafloor are necessarily localized, evaluating the proposition of serpentinites in the crust is an arduous ask [37]. If serpentinized peridotites, which are residual rocks from the mantle, crop out at the seafloor, this raises the question of the significance of the MOHO, classically interpreted as the transition between magmatic, mafic rocks and residual, ultramafic rocks (see Section 2) [34]. This sharp seismic boundary could correspond to a hydration front, i.e. the transition between partially serpentinized peridotites and fresh peridotites, corresponding to an increase in density. Because serpentinization occurs at temperatures below 500 °C, this hydration front may also correspond to a thermal boundary, i.e. the 500 °C isotherm [73].

The *magnetic properties* of ocean floor peridotites are also strongly affected by serpentinization because it produces secondary magnetite [52]. Therefore, compared to a fresh peridotite, a serpentinite has a high
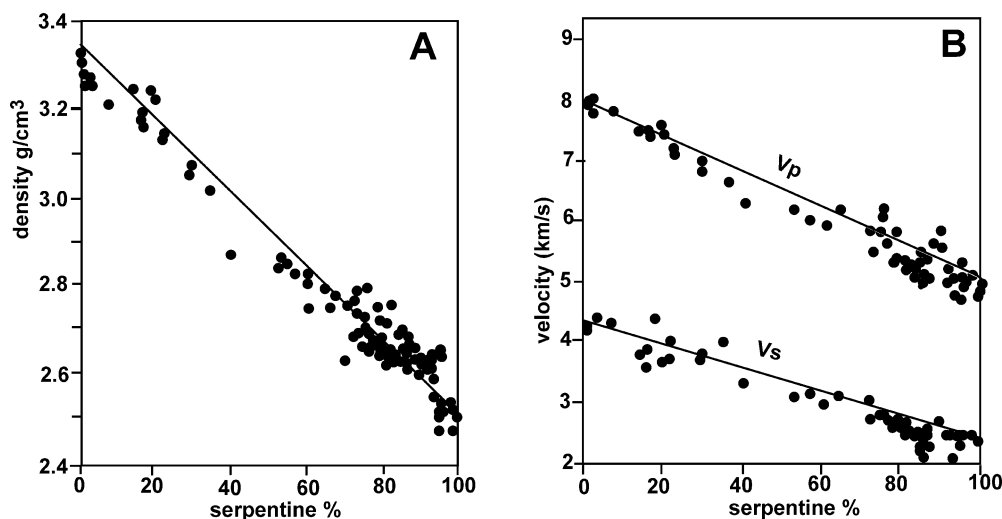

Fig. 8. Compilation of densities (**A**) and seismic velocities (**B**) measured on ocean floor serpentinites. Adapted from [99].

Fig. 8. Compilation des densités (**A**) et vitesses sismiques (**B**) mesurées dans les serpentinites océaniques. Adapté de [99].

magnetic susceptibility and a ferromagnetic behaviour [126]. Because of the crystallization of secondary magnetite, it also acquires a natural remanent magnetization (NRM) which can contribute to the magnetic anomalies of the seafloor [52]. At slow spreading ridges, it has been recognized that the off-axis traces of inside corner highs – massifs located at the intersection between a fracture zone and the ridge axis – are commonly marked by more positive magnetization, attributed to the occurrence of serpentinites [109,127]. Moreover, the skewness of magnetic anomalies on the seafloor has been ascribed to the contribution of serpentinized peridotites [53,54]. To interpret magnetization maps of the seafloor it is therefore essential to consider the possible presence of serpentinites.

A detailed study of the magnetic properties of oceanic serpentinites [108] has revealed the complexity of magnetite formation and how it affects the magnetic properties. The magnetic susceptibility is directly correlated to the amount of magnetite. However, this amount does not increase linearly with the rate of serpentinization as initially proposed [15] because the partitioning of iron between serpentine minerals and magnetite varies with the extent of serpentinization. The authors have shown that it remains modest at serpentinization rates below 75% because the iron partly enters serpentine minerals (up to 6% FeO). At higher serpentinization rates, the iron content of serpentine minerals decreases (2–3%) and more magnetite forms. They also show that the size of magnetite grains influences the NRM. The small sized magnetite grains associated with serpentine in mesh texture produce NRM as high as basalts. By contrast, in the case of large magnetite crystals, their occurrence as irregular aggregates likely promotes strong magnetostatic interactions between the grains and as a result reduces their coercitivity. Finally, low temperature oxidation of magnetite produces maghemite, and drastically decreases the magnetic susceptibility and NRM of serpentinites. In conclusion, this study confirms that serpentinites have generally high magnetic susceptibility and NRM and can contribute to magnetic anomalies. It demonstrates, however, that the modification in the magnetic properties of serpentinites is not linearly related to the rate of serpentinization. It is still necessary to better understand what controls the formation of magnetite to be able to predict the magnetic properties of the serpentinites peridotites in the ocean crust.

A last major effect of serpentinization concerns *rheology* which in turn affects the tectonic activity of the ocean lithosphere. Deformation experiments show that serpentinites, particularly when made of lizardite, are weaker than the other components of the oceanic lithosphere and display brittle deformation without dilatancy [55,56,112]. A small degree of serpentinization ($< 15\%$) reduces the strength of the peridotite to that of serpentine, while displaying the characteristic behaviour of pure serpentinites (e.g. non dilatant brittle deformation). The presence of lizardite-rich serpentinites in the crust may therefore strongly influence its strength and tectonics [55,57].

7. Serpentinization driven hydrothermal activity

The fact that serpentinization could affect the chemistry of the water column was first documented in the 1990s at the Mid-Atlantic Ridge. Specific anomalies, characterized by high methane concentrations together with low TDM (total dissolved manganese) contents and turbidity were identified and shown to be associated with serpentinite outcrops [39,40,42]. Serpentinization produces H_2 because of the oxidation of iron during the formation of magnetite using the oxygen from the aqueous fluid phase [64,101]. Calculated ultramafic hosted vent fluid compositions predict abundant H_2 concentrations, as opposed to basalt hosted vent fluids [131], in agreement with the observations. The production of methane is attributed to Fischer–Tropsch type reactions such as:

$$CO_2 + 4\,H_2 = CH_4 + 2\,H_2O$$
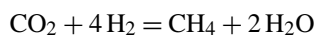
The formation of methane as well as other hydrocarbon components during serpentinization have been reproduced experimentally at 300 °C, 500 bars [10].

Further evidence for the existence of hydrothermal activity associated with serpentinites is the discovery of black smokers hosted on serpentinized peridotites. The Logatchev field was first discovered at 14°45′N latitude [17], followed by the Rainbow field at 36°14′N latitude [62] on the Mid-Atlantic Ridge. Although they are built on serpentinites, these two hydrothermal fields share a number of characteristics with hydrothermal fields hosted in basalts (Table 2),

Table 2
Comparison of fluid chemistry between hydrothermal vent fields from various ridge environments and seawater

Tableau 2
Comparaison de la chimie des fluides émis des endroits différents

	Logachev 1996	Rainbow 1997	Lost City 2001	TAG 1993	Seawater
Host rock	serpentinites	serpentinites	serpentinites	basalts	
Temperature	353	365 °C	40–75 °C	363 °C	2 °C
pH	2.8	3.3	8.0	3.1	7.8
H_2S mM	0.8	1.0	0.064	3–4	0
Mg mM	0	0	9–19	0	53
Na mM	438	553	479–485	550	464
Fe mM	2500	2400		5170	0.0045
Mn mM	330	2250		710	0.0013
Cl mM	515	750	546–549	650	546
Co mM	< 2	13		< 2	< 2
Ni mM	< 2	3.0		< 2	< 2
SO_4 mM			5.9–12.9		28.6
CH_4 mM		2.2	0.13–0.28	0.15–0.16	$\times 4 \times 10^{-7}$
H_2 mM		13	0.25–0.43	0.18–0.23	$\times 4 \times 10^{-4}$
	[51]	[51]	[82]	[51] except CH_4 and H_2 [41]	

and support biological communities. The fluids vent at high temperatures ($> 300\,°C$) and they build up sulfide chimneys. They have low pH, high H_2S and metal contents. However, they are characterized by high H^+ contents, consistent with the production of hydrogen during serpentinization [51]. Moreover, the presence of complex hydrocarbon molecules [75] – similar to those produced experimentally [10] – has been documented at Rainbow. This could be of great biological importance. Not only can methane support microbial communities [79,92], but also complex hydrocarbons are considered as prebiotic molecules which could have played a role in the appearance of life on Earth. There are some differences between the two fields, however. Hydrothermal fluids from the Rainbow field yield very high chlorinities, metal and REE concentrations, which could reflect phase separation [51]. Another field, the Saldanha hydrothermal field has also been discovered at 36°30N latitude on the Mid-Atlantic ridge, at the southern tip of the FAMOUS segment. Active vents discharge clear warm fluids through sediments, but no data on fluid compositions are yet available [11]. It should be pointed out that the black smoker type of vents generate turbidity in the water column. Therefore, they cannot account for the methane anomalies not associated with TDM

and turbidity documented in the water column [39] in the vicinity of serpentinite exposures.

The most recent discovery was the Lost City hydrothermal field [82]. This field is located off axis (1.5 Myear old crust) at 30°N, at the corner intersection between Atlantis fracture zone and the M.A.R. The fluids vent at low temperature (40–75 °C) and build spectacular hydrothermal chimneys (up to 60 m high) made up essentially of carbonates and brucite. The fluid compositions contrast with those from the Rainbow and Logachev sites (Table 2). In particular, they are characterized by high MgO and high pH, and low H_2S contents. The associated serpentinites indicate crystallization temperature of around 200 °C [66]. This field definitely differs from the two others both in temperature and chemistry of the fluids and associated deposits. Abundant microbial activity is associated with fluid venting and mineral precipitation [83]. In this case, the venting fluids could generate the methane anomalies not associated with turbidity that are commonly in the water column, in association with serpentinite outcrops.

Another evidence for hydrothermal activity was first documented by Bonatti et al. [29]. It consists of massive sepiolite deposits which are ascribed to the precipitation from a fluid phase resulting from

serpentinization. The same type of deposits occurs at the western portion of the SWIR [8]. The presence of sepiolite on the ocean floor could therefore be used as an indicator of serpentinization at depth.

Hydrothermal activity requires heat and different possible heat sources can be invoked [8]: (i) latent heat released by crystallization of basaltic magma intrusions in the lithospheric mantle; (ii) cooling heat mined from the lithospheric mantle; (iii) heat released by exothermic serpentinization reactions [69]. The question is whether the only heat released by serpentinization reactions can activate hydrothermal circulation and can account for fluid temperatures as high as 350 °C. Lowell and Rona [89] show that the heat released depends both on the serpentinization rate and the mass flow rate. They calculate that, in the absence of a regional background heat flux, serpentinization rates need to be very high (10^3 kg/s) and flow rates low (10 kg/s) to generate hydrothermal temperatures above 100 °C. Based on experimental diffusion rates, Mac Donald and Fyfe [90] evaluated that serpentinization rates are likely in the order of 0.1 kg/s. Even if this number can be increased if permeability generated by tectonic activity is considered, it remains extremely low compared to the value required. If a regional background heat flux is considered, the necessary rate of serpentinization decreases and becomes more realistic. But to generate hydrothermal temperatures of 300 °C, a high temperature regime, typical of magmatic systems at mid-ocean ridges is necessary. Lowell and Rona conclude that high temperature hydrothermal fields such as Rainbow require magmatic heat to drive the system. By contrast, the Lost City field can be driven by the heat released by serpentinization reactions. Provided that seawater can penetrate at depth, hydrothermal systems generated by serpentinization reactions are likely to be a significant component of hydrothermal activity at slow spreading ridges and generate anomalies in the water column. Bach et al. [8] came to the same conclusion. Assuming a heat capacity of seawater of 4 J g^{-1} K^{-1} and a water/rock ratio of 1, they calculate that serpentinization can heat up the circulating water by 25 to 150 °C. This can account for the range of temperatures measured at the Lost City type of hydrothermal field as well as for the formation of sepiolite deposits, but not for the Rainbow type of field.

These results suggest that black smoker vent fields (Rainbow type) can occur only at the ridge axis, where magmatic instrusions can provide heat to activate the hydrothermal circulation. Because the heat generated by serpentinization reactions can activate the Lost City type of vent field, such a type of hydrothermal activity can theoretically occur everywhere, either beneath the axial valley or off-axis. It only requires that seawater penetrates into unaltered peridotites. This can happen off-axis if tectonic activity generates permeability though fractures and faults. At this stage, we know that serpentinization is active at the axis since all the peridotites collected in the axial valley are serpentinized. However, we lack appropriate data to evaluate the intensity of off-axis serpentinization. Searching for methane and/or hydrogen anomalies in the water column off-axis would probably be the best strategy.

8. Conclusions

Recent developments on the understanding of the structure of mid-ocean ridges have demonstrated that serpentinites make up a significant portion of the seismically-defined crust. Therefore, the MOHO does not systematically correspond to the boundary between a magmatic crust and a residual mantle. In specific areas, particularly at the end of ridge segments generated in slow to ultraslow spreading environments, it may instead correspond to a hydration boundary, matching the 500 °C isotherm under the ridge axis. This has a major implication when evaluating the magmatic fluxes at mid-ocean ridges. The latter are clearly overestimated when the whole crustal thickness is considered. It is therefore of major importance to be able to quantitatively evaluate the proportion of serpentinized peridotites in the crust. Besides direct geological observation and sampling through dredging, diving and ocean drilling, it is necessary to develop tools, using indirect measurements such as seismic velocity profiles and/or magnetic properties.

Serpentinite fabrics show that most of the serpentinization occurs under static conditions. Determinations of serpentine species show the predominance of lizardite. By contrast, mineral associations as well as oxygen isotope fractionation demonstrate that serpentinization reactions start at high temperature, in the range of 300–500 °C, even if lower temperatures are also documented. This suggests that the nature of the

serpentine species may be controlled by factors other than temperature. High temperature serpentinization likely starts at depth, at the ridge axis, by interaction of seawater or seawater derived fluids with cooling peridotites. The lack of evidence for a massive leaching of major elements favours a compensation of the decrease in density by a volume increase. Because serpentinization requires a major flux of water, this raises the question of fluid penetration. The extensional environment must generate permeability through normal faulting, fissuring and cracking. At temperatures below 500 °C, the availability of water must be the limiting factor for extensive serpentinization.

The serpentinization of essentially anhydrous peridotites results in a massive hydration and oxidation. Major elements do not seem to be strongly affected by serpentinization, although the local rodingitization of associated gabbroic dikes and formation and talcshists require the mobilization of calcium and silicium. The global chemical fluxes between peridotite and seawater, however, remain poorly constrained. They seem to be dependent on the temperature and the mineral association. In particular, the presence and degree of alteration of pyroxene is likely of major importance, because this mineral concentrates a large part of the trace and REE of the fresh peridotite. In the present state of knowledge, it is safe to state that serpentinites are enriched in water, chlorine, fluorine, boron, sulfur, δ^{34}S, ^{87}Sr compared with fresh peridotites. The subduction of heterogeneous oceanic lithosphere does not only drive water but other elements, in particular halogens, into the mantle. These can affect arc magmatism through the dewatering of the suducting slab or be recycled in the mantle. Serpentinites must therefore be considered as one of the components of the subduction factory.

The presence of serpentinites strongly modifies the physical properties of the crust (density, seismic velocities, magnetic properties) and its rheology. To interpret geophysical data and tectonic fabrics in slow-spreading mid-ocean ridge environments, it is essential to keep in mind that serpentinites may be an important component of the oceanic crust.

Finally, hydrothermal circulation cells are associated with serpentinization. These can be identified by anomalies in the water column: methane anomalies associated with serpentinite outcrops in the axial valley likely document active serpentinization. The Rainbow type hydrothermal vent field with high temperature black smokers, however, seems to require a magmatic heat source. In contrast, the Lost City-type hydrothermal vent field could be generated by serpentinization reaction heat only. Biological activity, supported by the production of hydrogen and methane, is associated with active venting. The recent discovery of these hydrothermal fields stresses that serpentinization at mid-ocean ridges must be considered in thermal and geochemical budgets.

Acknowledgements

References

[1] P. Agrinier, R. Hékinian, D. Bideau, M. Javoy, O and H stable isotope of oceanic crust and upper mantle rocks exposed in the Hess Deep near the Galapagos triple junction, Earth Planet. Sci. Lett. 136 (1995) 183–196.

[2] P. Agrinier, M. Cannat, Oxygen isotopic constraints on serpentinization processes in ultramafic rocks from the Mid-Atlantic Ridge (23°N) in the MARK area, in: J.A. Karson, M. Cannat, D.J. Miller, D. Elthon (Eds.), Proc. ODP, Sci. Results, Vol. 153, College Station, TX, 1997, pp. 381–388.

[3] D.E. Allen, W.E. Seyfried, Compositional control on vent fluids from ultramafic hosted hydrothermal systems at mid-ocean ridges. An experimental study at 400 °C, 500 bars, Geochim. Cosmochim. Acta, in press.

[4] J.C. Alt, W.C.S. Shanks III, Sulfur in serpentinized oceanic peridotites: serpentinization processes, J. Geophys. Res. 103 (1998) 9917–9929.

[5] J.C. Alt, W.C.S. Shanks III, Serpentinization of abyssal peridotites from MARK area: sulfur reacti, Geochim. Cosmochim. Acta 67 (2003) 641–653.

[6] B. Anselmi, M. Mellini, C. Viti, Chlorine in Elba, Monti Livornesi and Murlo serpentinites: evidence for seawater interaction, Eur. J. Mineral. 12 (2000) 137–146.

[7] F. Aumento, H. Loubat, The Mid-Atlantic Ridge near 45°N: serpentinized ultramafic intrusions, Can. J. Earth Sci. 8 (1971) 631–663.

[8] W. Bach, N.R. Banerjee, H.J.B. Dick, E.T. Baker, Discovery of ancient and active hydrothermal systems along the ultra-slow spreading Southwest Indian Ridge 10–16°E, Geochem. Geophys. Geosyst. 3 (2002) 10.1029/2001GC000279.

[9] S.W. Bailey, Structures and compositions of other trioctahedral 1:1 phyllosilicates, in: Bailey (Ed.), Hydrous phyllosilicates other than micas, Rev. Mineral. 19 (1988) 169–188.

[10] E.A. Berndt, D.E. Allen, W.E.J. Seyfried, Reduction of CO_2 during serpentinization of olivine at 300 °C, Geology 24 (1996) 351–354.

[11] F.J.A.S. Barriga, Y. Fouquet, A. Almeida, M.J. Biscoto, J.L. Charlou, et al., Discovery of the Saldanha hydrothermal field on the FAMOUS segment of the Mid-Atlantic Ridge (36°30′N), EOS 79 (1998) 67.

[12] M.O. Beslier, M. Ask, G. Boillot, Ocean-continent boundary in the Iberian abyssal plain from multichannel seismic data, Tectonophysics 218 (1993) 383–393.

[13] M.O. Beslier, J.Y. Royer, P. Hill, E. Boeuf, C. Buchanan, F. Chatin, J. Girardeau, G. Jacovetti, A. Moreau, M. Munschy, C. Partouche, S. Thomas, U. Robert, Mantle exhumation at a rift zone; evidence for a wide ocean-continent transition along the Southwest Australian passive margin, EUG Conf. Abstracts EUG10 4 (1999) 377.

[14] D. Bideau, R. Hébert, R. Hékinian, M. Cannat, Metamorphism of deep seated rocks from the Garrett ultrafast transform (East Pacific Rise near 13°25′S), J. Geophys. Res. 96 (1991) 10079–10099.

[15] M. Bina, B. Henry, Magnetic properties, opaque mineralogy and magnetic anisotropies of serpentinized peridotites from Hole 670A near the Mid-Atlantic Ridge, Phys. Earth Planet. In. 65 (1990) 88–103.

[16] S.H. Bloomer, Distribution and origin of igneous rocks from the landward slopes of the Mariana Trench, implications for its structure and evolution, J. Geophys. Res. 88 (1983) 7411–7418.

[17] Y. Bogdanov, A.M. Sagalevitch, E.S. Chernayev, A.M. Ashadze, E.G. Gurvich, V.N. Lukashin, G.V. Ivanov, V.N. Peresypkin, A study of the hydrothermal field at 14°45′N on the Mid-Atlantic Ridge using the "MIR" submersibles, Bridge Newsletters 9 (1995) 9–13.

[18] G. Boillot, S. Grimaud, A. Mauffret, D. Mougenot, J. Mergoil-Daniel, J. Kornprobst, G. Torrent, Ocean-continent boundary off the Iberian margin: a serpentinite diapir west of the Galicia bank, Earth Planet. Sci. Lett. 48 (1980) 23–34.

[19] G. Boillot, E.L. Winterer, A.W. Meyer, in: Proceedings ODP, Init. Repts, Vol. 103, Ocean Drilling Program, College Station, TX, 1987.

[20] G. Boillot, J. Girardeau, J. Kornprobst, Rifting of the Galicia margin: crustal thinning and emplacement of mantle rocks on the seafloor, in: G. Boillot, E.L. Winterer (Eds.), Proceedings ODP Sci. Results, Vol. 103, Ocean Drilling Program, College Station, 1988, pp. 741–756.

[21] G. Boillot, G. Féraud, M. Recq, J. Girardeau, Undercrusting by serpentinites beneath rifted margins, Nature 341 (1989) 523–525.

[22] E. Bonatti, Ultramafic rocks from the Mid-Atlantic Ridge, Nature 219 (1968) 363–364.

[23] E. Bonatti, Serpentinite protrusions from the Mid-Atlantic Ridge, Earth Planet. Sci. Lett. 32 (1976) 107–113.

[24] E. Bonatti, Ancient continental mantle beneath oceanic ridges, J. Geophys. Res. 78 (1971) 3825–3831.

[25] E. Bonatti, J. Honnorez, G. Ferrara, Equatorial Mid-Atlantic Ridge: petrologic and Sr isotopic evidence for an alpine-type rock assemblage, Earth Planet. Sci. Lett. 9 (1970) 247–256.

[26] E. Bonatti, C. Emiliani, G. Ferrara, J. Honnorez, H. Rydell, Ultramafic carbonate breccias from the Equatorial Mid-Atlantic Ridge, Mar. Geol. 16 (1974) 83–102.

[27] E. Bonatti, J. Honnorez, Sections of the Earth's crust in the Equatorial Atlantic, J. Geophys. Res. 81 (1976) 4104–4116.

[28] E. Bonatti, P.R. Hamlyn, Oceanic ultramafic rocks, in: C. Emiliani (Ed.), The Sea, Vol. 7, Wiley and Sons, New York, 1981, pp. 241–283.

[29] E. Bonatti, E.C. Simmons, D. Breger, P.R. Hamlyn, J. Lawrence, Ultramafic rock/seawater interaction in the oceanic crust: Mg-silicate (sepiolite) deposit from the Indian Ocean floor, Earth Planet. Sci. Lett. 62 (1983) 229–238.

[30] E. Bonatti, J.R. Lawrence, N. Morandi, Serpentinization of oceanic peridotites: temperature dependence of mineralogy and boron, Earth Planet. Sci. Lett. 70 (1984) 88–94.

[31] E. Bonatti, M. Seyler, J. Channel, J. Girardeau, J. Mascle, Peridotites drilled from the Tyrrhenian sea, in: K.A. Kasten, J. Mascle (Eds.), Proceedings ODP Sci. Results, Vol. 107, Ocean Drilling Program, College Station, 1990, pp. 37–47.

[32] N.L. Bowen, O.F. Tuttle, The system MgO–SiO_2–H_2O, Geol. Soc. Am. Bull. 60 (1949) 439–460.

[33] J.R. Cann, D.K. Blackman, D.K. Smith, E. McAllister, B. Jannsen, S. Mello, E. Avgerinos, A.R. Pasco, J. Escartin, Corrugated slip surfaces formed at North Atlantic ridge-transform intersections, Nature 385 (1997) 329–332.

[34] M. Cannat, Emplacement of mantle rocks in the seafloor at mid-ocean ridges, J. Geophys. Res. 98 (1993) 4163–4172.

[35] M. Cannat, J.A. Karson, D.J. Miller, in: Proceedings ODP, Init. Repts, Vol. 53, Ocean Drilling Program, College Station, TX, 1994.

[36] M. Cannat, C. Mével, M. Maïa, C. Deplus, P. Gente, P. Agrinier, A. Belarouchi, G. Dubuisson, E. Humler, J.R. Reynolds, Thin crust, ultramafic exposure and rugged faulting patterns at the Mid-Atlantic Ridge (22°–24°N), Geology 23 (1995) 49–52.

[37] R.L. Carlson, The abundance of ultramafic rocks in the Atlantic ocean crust, Geophys. J. Int. 144 (2001) 37–48.

[38] L. Caruzo, J.V. Chernosky, The stability of lizardite, Can. Mineral. 17 (1979) 757–769.

[39] J.-L. Charlou, H. Bougault, P. Appriou, T. Nelsen, P. Rona, Different TDM/CH_4 hydrothermal plume signatures: TAG site at 26°N and serpentinized ultrabasic diapir at 15°05′N on the Mid-Atlantic Ridge, Geochim. Cosmochim. Acta 55 (1991) 3200–3322.

[40] J.-L. Charlou, J.-P. Donval, Hydrothermal methane venting between 12°N and 26°N along the Mid-Atlantic Ridge, J. Geophys. Res. 98 (1993) 9625–9642.

[41] J.-L. Charlou, J.-P. Donval, P. Jean-Baptiste, A. Dapoigny, P. Rona, Gases and helium isotopes in high temperature solutions sampled before and after ODP Leg 158 drilling at TAG hydrothermal field (26°N, MAR), Geophys. Res. Lett. 23 (1996) 3491–3494.

[42] J.-L. Charlou, Y. Fouquet, H. Bougault, J.-P. Donval, J. Etoubleau, P. Jean-Baptiste, A. Dapoigny, P. Appriou, P.A. Rona,

Intense CH$_4$ plumes generated by serpentinization of ultra-mafic rocks at the intersection of the 15°20′N fracture zone and the Mid-Atlantic Ridge, Geochim. Cosmochim. Acta 62 (1998) 2323–2333.

[43] N.I. Christensen, Elasticity of ultrabasic rocks, J. Geophys. Res. 71 (1966) 5921–5931.

[44] N.I. Christensen, The abundance of serpentinites in the oceanic crust, J. Geol. 80 (1972) 709–719.

[45] R.G. Coleman, A chemical study of serpentinization – Burro mountain, California, J. Petrol. 12 (1971) 311–328.

[46] M. Constantin, R. Hekinian, D. Ackermand, P. Stoffers, Mafic and Ultramafic Intrusions into Upper Mantle Peridotites from Fast Spreading Centers of the Easter Microplate (South East Pacific), in: R.L.M. Vissers, A. Nicolas (Eds.), Mantle and Lower Crust Exposed in Ocean Ridges and Ophiolites, Kluwer Academic Publishing, Dordrecht, 1995, pp. 71–120.

[47] S. Decitre, E. Deloule, L. Reisberg, R. James, P. Agrinier, C. Mével, Behavior of Li and its isotopes during serpentinization of oceanic peridotites, Geochem. Geophys. Geosyst. (2001) 10.1029/2001GC000178.

[48] R. Detrick, J. Honnorez, W.B. Bryan, T. Juteau, in: Proceedings ODP, Init. Repts, Vols. 106/109, Ocean Drilling Program, College Station, TX, 1988.

[49] H.J.B. Dick, Abyssal peridotites, very spreading ridges and ocean ridge magmatism, in: A.D. Saunders, M.J. Norry (Eds.), Magmatism in the Ocean Basins, Blackwell, Malden, MA, 1989, pp. 71–105.

[50] Y. Dilek, A. Coulton, S.D. Hurst, Serpentinization and hydrothermal veining in peridotites at site 920 in the MARK area, in: J.A. Karson, M. Cannat, D. Elthon (Eds.), Proceedings ODP, Sci. Results, Vol. 153, College Station, TX, 1997, pp. 35–59.

[51] E. Douville, J.-L. Charlou, E.H. Oelkers, P. Bienvenu, C.F.J. Colon, J.P. Donval, Y. Fouquet, D. Prieur, P. Appriou, The Rainbow vent fluid (36°14′N, MAR): the influence of ultramafic rocks and phase separation on trace metal content in Mid-Atlantic Ridge hydrothermal fluids, Chem. Geol. 184 (2002) 37–48.

[52] D.J. Dunlop, M. Prévôt, Magnetic properties and opaque mineralogy of drilled submarine rocks, Geophys. J. R. Astron. Soc. 7 (1982) 709–757.

[53] J. Dyment, J. Arkani-Hamed, Spreading-rate dependent magnetization of the oceanic lithosphere inferred from the anomalous skewness of marine magnetic anomalies, Geophys. J. Int. 121 (1995) 789–804.

[54] J. Dyment, J. Arkani-Hamed, A. Ghods, Contribution of serpentinized ultramafics to marine magnetic anomalies at slow and intermediate spreading centers: insights from the shape of the anomalies, Geophys. J. Int. 129 (1997) 691–701.

[55] J. Escartin, B. Hirth, B. Evans, Nondilatant brittle deformation of serpentinites: implications for Mohr-Coulomb theory and the strenght of faults, J. Geophys. Res. 102 (1997) 2897–2913.

[56] J. Escartin, G. Hirth, B. Evans, Effects of serpentinization on the lithosphere strength and the style of normal faulting at slow spreading ridges, Earth Planet. Sci. Lett. 151 (1997) 181–190.

[57] J. Escartin, G. Hirth, B. Evans, Strength of slightly serpentinized peridotites: implications for the tectonics of oceanic lithosphere, Geology 29 (2001) 1023–1026.

[58] J. Escartin, C. Mével, C.J. MacLeod, A. McCaig, Constraints on the origin of detachments and deformation conditions: the Mid-Atlantic Ridge core complex at 15°45′N, Geochem. Geophys. Geosyst., Vol. 4, N° 8, 1067, doi:10.1029/2002GC000472.

[59] B.W. Evans, W. Johannes, H. Otterdoom, V. Trommsdorff, Stability of chrysotile and antigorite in the serpentine multi-system, Schweiz. Mineral. Petrogr. Mitt. (1976) 79–93.

[60] J. Ewans, J. Hawkins, Petrology of "seamounts" on the trench slope break, EOS 60 (1979) 968.

[61] R.L. Fisher, C.G. Engel, Ultramafic and basaltic rocks dredged from the near-shore flank of the Tonga trench, Geol. Soc. Am. Bull. 80 (1969) 1373–1378.

[62] Y. Fouquet, J.-L. Charlou, H. Ondréas, J. Radford-Knoery, J.-P. Donval, E. Douville, R. Apprioual, P. Cambon, H. Pell, J.-Y. Landur, A. Normand, E. Ponsevera, C. German, L. Parson, F. Barriga, I. Costa, J. Relvas, A. Ribeiro, Discovery and first submersible investigations on the Rainbow hydrothermal field on the MAR (36°14′N), EOS (1997) 832.

[63] J. Francheteau, R. Armijo, J.-L. Cheminée, R. Hékinian, P. Lonsdale, N. Blum, 1 My East Pacific Rise oceanic crust and uppermost mantle exposed by rifting in Hess Deep (equatorial Pacific Ocean), Earth Planet. Sci. Lett. 101 (1990) 281–296.

[64] R. Frost, On the stability of sulfides, oxides and native metals in serpentinite, J. Petrology 26 (1985) 31–63.

[65] G. Früh-Green, A. Plas, C. Lécuyer, Petrologic and stable isotope constraints on hydrothermal alteration and serpentinization of the EPR shallow mantle at Hess Deep (Site 895), in: C. Mével, K.M. Gillis, J.F. Allan, P.S. Meyer (Eds.), Proceedings of the ODP, Sci. Results, Vol. 147, College Station, TX, 1996.

[66] G. Früh-Green, C. Boschi, D.S. Kelley, J.A.D. Connolly, M.O. Schrenk, The role of serpentinization in metasomatism, carbonate precitpitation and microbial activity: stable isotope constraints from the Lost City vent field (MAR 30°N), EOS 83 (2002) 1451.

[67] P. Fryer, G.F. Fryer, Origin of non-volcanic seamounts in a forearc environment, in: B. Keating, P. Fryer, R. Batiza (Eds.), Seamounts, Islands and Atolls, Geophys. Monogr. Series, Vol. 43, Am. Geophys. Union, 1987, pp. 61–69.

[68] P. Fryer, J.A. Pearce, L.B. Stokking, in: Proc. ODP, Init. Repts, Vol. 125, Ocean Drilling Program, College Station, TX, 1990.

[69] W.S. Fyfe, P. Lonsdale, Ocean floor hydrothermal activity, in: C. Emiliani (Ed.), The Sea, Vol. 7, Wiley and Sons, New York, 1981, pp. 589–638.

[70] K.R. Gillis, C. Mével, J.F. Allen, in: Proceeding ODP, Init. Repts, Vol. 53, Ocean Drilling Program, College Station, TX, 1993.

[71] E. Gracia, J.-L. Charlou, J. Radford-Knoery, L.M. Parson, Non transform offsets along the Mid-Atlantic Ridge south of the Azores (38°N–34°N): ultramafic exposures and hosting of hydrothermal vents, Earth Planet. Sci. Lett. 177 (2000) 89–103.

[72] B. Grobety, A. Plas, G. Früh-Green, Serpentinization temperature of ocean floor peridotites from the Hess Deep rift valley, Pacific Ocean, Terra Nova 9 (1997) 549.

[73] H.H. Hess, History of the ocean basins, in: Petrologic Studies, Buddington Volume, Geological Society of America, Boulder, CO, 1962, pp. 599–620.

[74] R. Hébert, A.C. Adamson, S.C. Komor, Metamorphic petrology of ODP Leg 109, Hole 670A, serpentinized peridotites: serpentinization processes at a slow spreading ridge environment, in: R. Detrick, J. Honnorez, W.B. Bryan, T. Juteau (Eds.), Proceedings ODP, Sci. Results, Vols. 106–109, College Station, TX , 1990, pp. 103–113.

[75] N.G. Holm, J.-L. Charlou, Initial indications of abiotic formation of hydrocarbons in the Rainbow ultramafic hydrothermal system, Mid-Atlantic Ridge, Earth Planet. Sci. Lett. 191 (2001) 1–8.

[76] J. Honnorez, P. Kirst, Petrology of rodingites from the equatorial Mid-Atlantic fracture zones and their geotectonic significance, Contrib. Mineral. Petrol. 49 (1975) 233–257.

[77] H. Horen, M. Zamora, G. Dubuisson, Seismic wave velocities and anisotropy in serpentinized peridotites from Xigaze ophiolite: abundance of serpentine at slow-spreading ridges, Geophys. Res. Lett. 23 (1996) 9–12.

[78] D.R. Janecky, W.E. Seyfried, Hydrothermal serpentinization of peridotite within the oceanic crust: experimental investigations of mineralogy and major element chemistry, Geochim. Cosmochim. Acta 50 (1986) 1357–1378.

[79] H.W. Jannash, Microbial interactions with hydrothermal fluids, in: S.E. Humphris, et al. (Eds.), Seafloor Hydrothermal Systems: Physical, Chemical, Biological and Geological Interactions, Am. Geophys. Union, Washington, DC, 1995, pp. 273–296.

[80] P. Jean-Baptiste, J.-L. Charlou, M. Stievenard, Oxygen isotope study of mid-ocean ridge hydrothermal fluids: implication for the oxygen-18 budget of the oceans, Geochim. Cosmochim. Acta 61 (1997) 2669–2677.

[81] J.A. Karson, G. Thompson, S.E. Humphris, J.M. Edmonds, W.B. Bryan, J.R. Brown, A.T. Winters, R.A. Pockalny, J.F. Casey, A.C. Campbell, G. Klinkhammer, M.R. Palmer, R.J. Kinzler, M.M. Sulanowska, Along axis variation in seafloor spreading in the MARK area, Nature 328 (1987) 681–685.

[82] D.S. Kelley, J.A. Karson, D.K. Blackman, G.L. Früh-Green, D.A. Butterfield, M.D. Lilley, E.J. Olson, M.O. Shrenk, K.K. Roe, G.T. Lebon, P. Rivizzigno, An off-axis hydrothermal vent field discovered near the Mid-Atlantic Ridge at 30°N, Nature 412 (2001) 145–149.

[83] D.S. Kelley, J.A. Baross, G.L. Früh-Green, M.O. Shrenk, J.A. Karson, The ultramafic-hosted Lost City hydrothermal field: clues in the search for life elsewhere in the solar system, EOS (2002) 222.

[84] K.L. Kimball, F.S. Spear, H.J.B. Dick, High temperature alteration of abyssal ultramafics from the Islas Orcadas Fracture Zone, South Atlantic, Contrib. Mineral. Petrol. 91 (1985) 307–320.

[85] K.L. Kimball, D.C. Gerlach, Sr isotopic constraints on hydrothermal alteration of ultramafic rocks in two oceanic fracture zones from the South Atlantic ocean, Earth Planet. Sci. Lett. 78 (1986) 177–188.

[86] S.C. Komor, D. Elthon, J.F. Casey, Serpentinization of cumulate ultramafic rocks from the North Arm Mountain massif of the Bay of Islands ophiolite, Geochim. Cosmochim. Acta 49 (1985) 2331–2338.

[87] S.C. Komor, T.L. Grove, R. Hébert, Abyssal peridotites from ODP Hole 670A (21°10′N, 45°02′W): residues of mantle melting exposed by non contructive axial divergence, in: R.S. Detrick, J. Honnorez, W.B. Bryan, T. Juteau (Eds.), Proceedings ODP, Sci. Results, Vols. 106–109, College Station, TX, 1990, pp. 85–101.

[88] Y. Lagabrielle, D. Bideau, M. Cannat, J.A. Karson, C. Mével, Ultramafic-mafic plutonic rock suites exposed along the Mid-Atlantic Ridge (10–30°N). Symmetrical-asymmetrical distribution and implications for seafloor spreading processes, in: W.R. Buck, P.T. Delaney, J.A. Karson, Y. Lagabrielle (Eds.), Faulting and Magmatism at Mid-Ocean Ridges, in: Volume Geophysical Monograph, Vol. 106, AGU, Washington, DC, 1998, pp. 153–176.

[89] R.P. Lowell, P.A. Rona, Seafloor hydrothermal systems driven by the serpentinization of peridotite, Geophys. Res. Lett. 29 (2002) 10.1029/2001GL014411.

[90] A.H. MacDonald, W.S. Fyfe, Rate of serpentinization in seafloor environments, Tectonophysics 116 (1985) 123–135.

[91] C.J. MacLeod, J. Escartín, G.J. Banks, D.H.B. Irving, R.M. Lilly, Y.-L. Niu, D. Banerji, A. McCaig, S. Allerton, D.K. Smith, Direct geological evidence for oceanic detachment fauling: The Mid-Atlantic Ridge, 15°45′N, Geology 30 (2002) 879–882.

[92] T. McCollom, E.L. Shock, Geochemical constraints on chemolithoautrophic metabolism by microorganisms in seafloor hydrothermal systems, Geochim. Cosmochim. Acta 61 (1997) 4375–4391.

[93] B. Martin, W.S. Fyfe, Some experimental and theoretical observations on the kinetics of hydration reactions with particular reference to serpentinization, Chem. Geol. 6 (1970) 185–195.

[94] M. Mellini, P.F. Zanazzi, Crystal structure of lizardite-1T and lizardite 2H1 from Coli, Italy, Am. Mineral. 72 (1987) 943–948.

[95] M.A. Menzies, A. Long, G. Ingram, M. Tatnell, D. Janecky, MORB peridotite-seawater interaction: experimental constraints on the behaviour of trace ellements, $^{87}Sr/^{86}Sr$ and $^{143}Nd/^{144}Nd$ ratios, in: H.M. Prichard, T. Alabaster, N.B.W. Harris, C.R. Neary (Eds.), Magmatic Processes and Plate Tectonics, in: Geological Society Special Publication, Vol. 76, 1993, pp. 309–322.

[96] C. Mével, C. Stamoudi, Hydrothermal alteration of the upper mantle section at Hess Deep, in: C. Mével, K. Gillis, J. Allan (Eds.), Proceedings of the ODP, Sci. Res., Vol. 147, College Station, TX, 1996, pp. 293–309.

[97] C. Mével, the EDUL Scientific Party, Sampling the South West Indian Ridge: first results of the EDUL cruise (R/V Marion Dufresne), InterRidge News 6 (1997) 25–26.

[98] P. Michael, J. Thiede, H.J.B. Dick, S.L. Goldstein, D. Graham, W. Jokat, C.H. Langmuir, R. Muhe, J.E. Snow, The Arc-

tic Mid-Ocean Ride Expedition – AMORE 2002 – Seafloor spreading at the top of the world, EOS 82 (2001) 1097.

[99] D.J. Miller, N.I. Christensen, Seismic velocities of lower crustal and upper mantle rocks from the slow-spreading Mid-Atlantic Ridge, South of the Kane transform zone (MARK area), in: J.A. Karson, M. Cannat, D.J. Miller, D. Elthon (Eds.), Proc. ODP, Sci. Results, Vol. 153, College Station, TX, 1997.

[100] A. Miyashiro, F. Shido, M. Ewing, Composition and origin of serpentinites from the Mid-Atlantic Ridge near 24 and 30°N, Contrib. Mineral. Petrol. 23 (1969) 117–127.

[101] J.B. Moody, Serpentinization: a review, Lithos 9 (1976) 125–138.

[102] I.A. Nicholls, J. Ferguson, H. Jones, G.P. Marks, J.C. Mutter, Ultramafic blocks from the ocean floor southwest of Australia, Earth Planet. Sci. Lett. 56 (1981) 362–374.

[103] D.S. O'Hanley, Solution to the volume problem in serpentinization, Geology 20 (1992) 705–708.

[104] D.S. O'Hanley, Serpentinites, Oxford University Press, New York, 1996, 277 pp.

[105] D.S. O'Hanley, F.J. Wicks, Conditions of formation of lizardite, chrysotile and antigorite, Cassiar, British Columbia, Can. Mineral. 33 (1995) 753–773.

[106] D.S. O'Hanley, J.V. Chernovsky Jr, F.J. Wicks, The stability of lizardite and chrysotile, Can. Mineral. 27 (1989) 483–493.

[107] B. Orberger, N. Métrich, M. Mosbach, C. Mével, Y. Fouquet, Nuclear microprobe analysis of serpentine from the Mid-Atlantic Ridge, Nucl. Instrum. Meth. B 158 (1999) 575–581.

[108] O. Oufi, M. Cannat, H. Horen, Magnetic properties of variably serpentinized abyssal peridotites, J. Geophys. Res. 107 (2002) 1–19.

[109] J.E. Pariso, C. Rommevaux, J.C. Sempéré, Three dimensional inversion of marine magnetic anomalies: implications for crustal accretion along the Mid-Atlantic Ridge (28°–31°30′N), Marine Geophys. Res. 18 (1996) 85–101.

[110] PENROSE, Ophiolites, Geotimes (1972) 24–25.

[111] H.M. Prichard, A petrographic study of the process of serpentinization in ophiolites and the ocean crust, Contrib. Mineral. Petrol. 68 (1979) 231–241.

[112] C.B. Raleigh, M.S. Paterson, Experimental deformation of serpentinites and its tectonic implication, J. Geophys. Res. 70 (1965) 3865–3985.

[113] R. Sakai, M. Kusakabe, M. Noto, T. Ishii, Origin of water responsible for serpentinization of Izu–Ogasawara–Marianna forearc seamounts in view of H and O isotopes, Earth Planet. Sci. Lett. 100 (1990) 291–303.

[114] W.E. Seyfried, W.E. Dibble, Seawater-peridotite interaction at 300 °C and 500 bars: implications for the origin of oceanic serpentinites, Geochim. Cosmochim. Acta 44 (1980) 309–321.

[115] W.C. Shanks III, Stable isotopes in seafloor hydrothermal systems: vent fluids, hydrothermal deposits, hydrothermal alteration and microbial processes, in: J.M. Valley, R. Cole (Eds.), Reviews in Mineralogy and Geochemistry, Vol. 41, 2001, pp. 469–525.

[116] S.M.F. Sheppard, Isotopic evidence for the origins of water during metamorphic processus in oceanic crust and ophiolite complexes, Coll. Int. CNRS 272 (1980) 135–147.

[117] J. Sinton, R.S. Detrick, Mid-ocean ridge magma chambers, J. Geophys. Res. 97 (1992) 197–216.

[118] J.E. Snow, S. Hart, H.J.B. Dick, "Orphan" strontium-87 in abyssal peridotites: daddy was a granite, Science 262 (1993) 1861–1863.

[119] J.E. Snow, H.J.B. Dick, Pervasive magnesium loss by marine weathering of peridotites, Geochim. Cosmochim. Acta 59 (1995) 4219–4235.

[120] J.E. Snow, L. Reisberg, Os isotopic systematics of MORB mantle: results from altered abyssal peridotites, Earth Planet. Sci. Lett. 136 (1995) 723–733.

[121] C. Stamoudi, Processus de serpentinisation des péridotites de Hess Deep et de la zone MARK, unpublished thesis, Université Pierre et Marie Curie, Paris (2002) 372 pp.

[122] A.M. Steuber, W.H. Huang, W.D. Johns, Chlorine and fluorine in ultramafic rocks, Geochim. Cosmochim. Acta 32 (1968) 353–358.

[123] K. Tamaki, C. Mével and the FUJI scientific Party, Spreading Tectonics of the Eastern part of the Southwestern Indian Ridge: a Synthesis of FUJI Expedition, EOS 79 (1998) 892.

[124] P. Tartarotti, M. Cannat, C. Mével, Gabbroic dikelets in serpentinized peridotites from the Mid-Atlantic ridge at 23°20′N, in: R.L.M. Vissers, A. Nicolas (Eds.), Mantle and Lower Crust Exposed in Ocean Ridges and Ophiolites, Kluwer Academic Publishing, Dordrecht, 1995, pp. 35–69.

[125] G. Thompson, W.G. Melson, Boron contents of serpentinites and metabasalts in the oceanic crust: implications for the boron cycle in the ocean, Earth Planet. Sci. Lett. 62 (1970) 229–238.

[126] P.B. Toft, J. Arkani-Hamed, S.E. Haggerty, The effect of serpentinization on density and magnetic susceptibility, Phys. Earth Planet. In. 65 (1990) 137–157.

[127] B. Tucholke, J. Lin, A geological model for the structure of ridge segments in slow spreading ocean crust, J. Geophys. Res. 99 (1994) 11937–11958.

[128] S. Uehara, H. Shirozu, Variations in chemical compositions and structural properties of antigorite, Mineral. J. 12 (1985) 299–318.

[129] D.B. Wenner, H.P. Taylor, Temperatures of serpentinization of ultramafic rocks based on $^{18}O/^{16}O$ fractionation between coexisting serpentine and magnetite, Contrib. Mineral. Petrol. 32 (1971) 165–185.

[130] D.B. Wenner, H.P. Taylor, Oxygen and hydrogen isotope studies of serpentinization of ultramafic rocks in oceanic environments and continental ophiolite complexes, Am. J. Sci. 273 (1973) 207–239.

[131] L.R. Wetzel, E.L. Shock, Distinguishing ultramafic- from basalt-hosted submarine hydrothermal systems by comparing calculated vent fluid compositions, J. Geophys. Res. 105 (2000) 8319–8340.

[132] F.J. Wicks, E.J.W. Wittacker, A reappraisal of the structure of serpentine minerals, Can. Mineral. 13 (1975) 227–243.

[133] F.J. Wicks, D.S. O'Hanley, Serpentine minerals: structure and petrology, in: Reviews in Mineralogy, Vol. 19, Min. Soc. America, 1988, pp. 91–167.

[134] R.B. Witmarsh, M.O. Beslier, P. Wallace, in: Proceedings ODP, Init. Repts, Vol. 149, Ocean Drilling Program, College Station, TX, 1993.